arXiv:1611.06452v1 [math.NA] 19 Nov 2016

MODEL REDUCTION FOR CALIBRATION OF AMERICAN OPTIONS

O. BURKOVSKA, K. GLAU, M. MAHLSTEDT, AND B. WOHLMUTH

Abstract. American put options are among the most frequently traded single stock options, and their calibration is computationally challenging since no closed-form expression is available. Due to the higher flexibility in comparison to European options, the mathematical model involves additional constraints, and a variational inequality is obtained. We use the Heston stochastic volatility model to describe the price of a single stock option. In order to speed up the calibration process, we apply two model reduction strategies. Firstly, a reduced basis method (RBM) is used to define a suitable low-dimensional basis for the numerical approximation of the parameter-dependent partial differential equation (μPDE) model. By doing so the computational complexity for solving the μPDE is drastically reduced, and applications of standard minimization algorithms for the calibration are significantly faster than working with a high-dimensional finite element basis. Secondly, so-called de-Americanization strategies are applied. Here, the main idea is to reformulate the calibration problem for American options as a problem for European options and to exploit closed-form solutions. Both reduction techniques are systematically compared and tested for both synthetic and market data sets.

1. Introduction

Mathematical models for option pricing typically depend sensitively on a set of parameters such as, e.g., the interest rate, the long-run variance, the rate of mean reversion, the volatility of volatility and the correlation parameter. Reliable predictions are only possible if these parameters are known. While the interest rate is often known a priori, other parameters cannot be accessed directly from the observed market data but have to be determined by a computationally challenging calibration process. Constantly changing market situations then require fast parameter fitting algorithms. Here, we consider single stock options of American type. This type of options is path-dependent, as the option holder has the right to exercise it at any time until maturity. Moreover, it is one of the most popular choices to be traded at exchange stocks. To be able to react instantaneously to market movements, complexity reduction techniques are of special interest. Both European and American options can be based on a parameter-dependent partial differential equation in time and asset price, see, e.g., [2, 34] and the references therein. However due to the higher flexibility of exercising American options compared to European options, the mathematical model for an American model has to be enriched by a suitable inequality constraint, reflecting the arbitrage-free principle. Then the problem under consideration can be reformulated as a weak variational inequality problem to which semi-smooth Newton schemes can be applied as non-linear solvers. Classical finite discretization schemes such as finite elements or finite differences then require rather high-dimensional basis spaces leading to large systems to

Date: November 22, 2016.

Key words and phrases. Reduced basis method, model reduction, American option, calibration, Heston model, de-Americanization.

This work was partly supported by: DFG grant WO671/11-1; International Research Training Group IGDK1754, funded by the German Research Foundation (DFG) and the Austrian research fund (FWF); KPMG Center of Excellence in Risk Management.

be solved. To reduce the computational cost, we apply two different reduction techniques. The first is based on reduced basis methods, which are perfectly suitable for parameter-dependent partial differential equations, while the second exploits the fact that closed-form solutions can be accessed for the simpler European options. The key idea of the reduced basis method is to replace the locally supported standard FEM basis functions by basis functions formed by solutions of the μPDE with specific choices of parameters. By doing so, we typically obtain dense algebraic systems of considerably smaller size.

The RBM is not a new approach and has been extensively studied in the literature for a wide range of applications, see, e.g., [45, 50, 32] and the references therein. However, little attention has been paid to applications in finance. Recent work on model reduction techniques in finance with a primary focus on POD methods include, e.g., [58, 56, 57, 49, 46]. First results for RBM can be found in [16, 48, 49]. In [43], RBM was applied to more complex models, e.g., with parameter functions as an initial condition. While these references focus on the simplest case of European options, American options, which are described by parabolic variational inequalites, are considered in [12, 10, 5]. In the case of parabolic variational inequalities, appropriately constructing the reduced basis spaces is much more challenging than for variational equalities. To tackle this, POD-Angle-Greedy strategies [12] or non-negative matrix factorization algorithms [4, 5] can be used. We also mention the relevant works on RBM for variational inequalities for the stationary case [31, 64] and instationary case in a space-time framework, e.g., [26].

Option pricing is associated with the calibration of non-observable parameters. This task can be formulated as a least-squares minimization problem, which finds a model parameter that minimizes the discrepancy between the model and market option prices in the sense of least squares. These problems typically require require the numerical solution of the μPDE to be evaluated many times for different values of the parameter, which incurs to a high computational cost. Therefore, to accelerate the calibration routine while still providing accurate results, we aim to apply the RBM. The idea is to replace the complex PDE model by a simpler surrogate model constructed by the RBM approaches, or alternatively by POD techniques, e.g., [56, 57]. Whereas calibration with the RBM in the linear case of European options has already been studied in the literature [16, 47], the extension to American options, to the best of our knowledge, has not yet been addressed. We also mention the application of the RBM to PDE-constrained optimization problems [59] using the POD method and recent work [19] on the reduced basis method.

The calibration problem can be also studied in the context of the theory of inverse problems. Most works are concerned with reconstructing the implied volatility surface for European options in the Black-Scholes model. This leads to an infinite-dimensional ill-posed inverse problem. We refer, e.g., to [7], where unique solvability and stability of the inverse problem are analyzed, and to [21], where an appropriate Tychonov regularization strategy is proposed to address the inherent ill-posedness of the problem. Similarly, in [1, 3], an infinite-dimensional Tychonov regularized problem for American options is considered and the existence of solutions is derived together with their optimality conditions. In the present case, due to the finite-dimensional parameter space, we generally expect the corresponding inverse problem to be well-posed, and so we do not use a regularization term.

We note that for calibration one can also work directly in the stochastic framework and compute the model prices, e.g., using a Monte-Carlo method by applying a backward regression scheme as in [42] or by using different Monte-Carlo estimates as in e.g. [9, 24, 52]. Alternatively one can apply (binomial) tree methods as e.g. in [18, 55]. For European options, closed-form solutions can be used, or FFT techniques, see, e.g., [44, 61, 25]. Fourier

transform based pricing methods have been extended to price American options, see for instance [22] and [41]. These methods are applicable when the Fourier transform of the modelling stochastic process evaluated at fixed times is available in closed-form. In this article we focus on a PDE-based approach that has a more general scope.

Whereas discretization techniques for PDEs and RDMs form a rather flexible and abstract framework, de-Americanization strategies are specially designed for the valuation of American options [13, 11]. These strategies first transform the price into a pseudo-European option price and secondly calibrate the European option by directly applying the computationally less expensive closed-form solution. In [11], the de-Americanization techniques are studied numerically, which also reveals their limitations. Both model reduction techniques, i.e., the RBM strategy and the de-Americanization strategy, are numerically studied and compared for the Heston model [33].

The rest of the paper is structured as follows: The model problem and the calibration procedure is briefly introduced in 3. In Section 4, we discuss a POD-Angle-Greedy RBM for the variational inequality of an American option pricing problem based on the Heston model. Section 5 is devoted to the surrogate model obtained by the de-Americanization strategy (DAS). In Section 6 both RBM and DAS are investigated numerically. A comparative study of both techniques is presented in Section 6.3. Here, we use synthetic as well as real market data sets to calibrate the unknown parameters.

2. Model problem

To calculate the price of an option (European or American) in a specific model, suitable data must be provided. These data consist of the current asset price $S_0 > 0$, the maturity time $T > 0$, the strike price $K > 0$, and the set of input parameters, which are denoted by the vector $\boldsymbol{\mu} \in \mathcal{P}$, where $\mathcal{P} \subset \mathbb{R}^p$ is a parameter domain. Whereas the first three components, S_0, K, T, are known and provided by the market data, the input parameter vector $\boldsymbol{\mu}$ is not known a priori, except for the interest rate $r > 0$, and needs to be estimated from the market. These types of problems are referred to as parameter identification or calibration problems. That is, given a set of observations of market option prices, we are interested in the parameter $\boldsymbol{\mu}$ that provides the best fit to the observed market data.

Generally, the market data is characterized by the actual spot price S_0 and the market option prices $P_i^{\text{obs}} = P^{\text{obs}}(S_0, T_i, K_i)$ for different maturities T_i and for different strikes K_i, $i = 1, \dots, M$. Mathematically, the calibration of option prices can be stated as a least squares minimization problem: find $\boldsymbol{\mu} \in \mathcal{P}_{\text{opt}} \in \mathcal{P}$ that solves

$$\min_{\boldsymbol{\mu}} J(\boldsymbol{\mu}), \qquad J(\boldsymbol{\mu}) := \frac{1}{M} \sum_{i=1}^{M} |P_i^{\text{obs}} - P_i(\boldsymbol{\mu})|^2, \tag{2.1}$$

where $P_i(\boldsymbol{\mu}) = P(S_0, T_i, K_i; \boldsymbol{\mu})$ are the model prices, which can for example be computed by solving the associated μPDE. More precisely, for European options, $P_i(\boldsymbol{\mu})$ solves

$$\frac{\partial P_i(\boldsymbol{\mu})}{\partial \tau} + \mathcal{L}(\boldsymbol{\mu}) P_i(\boldsymbol{\mu}) = 0, \qquad \text{in} \quad [0, T) \times \mathbb{R}_+^n, \tag{2.2a}$$

$$P(T_i; \boldsymbol{\mu}) = \mathcal{H}_i, \qquad \text{in} \quad \mathbb{R}_+^n, \tag{2.2b}$$

where $\mathcal{H}_i$ is a pay-off functional and $\mathcal{H}_i = (K_i - S)_+$ for the put and $\mathcal{H}_i = (S - K_i)_+$ for the call options, $n = 1, 2$, and τ denotes the time to maturity $T := \max(T_i)$, $i = 1, \dots, M$.

In the case of American put options, $P_i(\boldsymbol{\mu})$ satisfies

$$\frac{\partial P_i(\boldsymbol{\mu})}{\partial \tau} + \mathcal{L}(\boldsymbol{\mu})P_i(\boldsymbol{\mu}) \leq 0, \qquad \text{in} \quad [0,T) \times \mathbb{R}^n_+, \tag{2.3a}$$

$$P_i(\boldsymbol{\mu}) \geq \mathcal{H}_i, \qquad \text{in} \quad [0,T) \times \mathbb{R}^n_+, \tag{2.3b}$$

$$\left(\frac{\partial P_i(\boldsymbol{\mu})}{\partial \tau} + \mathcal{L}(\boldsymbol{\mu})P_i(\boldsymbol{\mu})\right)(P_i(\boldsymbol{\mu}) - \mathcal{H}_i) = 0, \qquad \text{in} \quad [0,T) \times \mathbb{R}^n_+, \tag{2.3c}$$

$$P(T_i;\boldsymbol{\mu}) = \mathcal{H}_i, \qquad \text{in} \quad \mathbb{R}^n_+, \tag{2.3d}$$

with $\mathcal{H}_i := (K_i - S)_+$. Both problems are subject to suitable boundary conditions. The operator $\mathcal{L}$ is a spatial (integro-) differential operator and is defined by the model used to price the option, e.g., Black-Scholes [6], CEV model, Heston [33]. Here, we restrict ourselves to the Heston model, [25, 44, 61], due to its ability to replicate the market behavior better than some other models.

3. The Heston model and its calibration

We continue our discussion by introducing the Heston model [33], which is used to calibrate the option prices, and and by describing the calibration procedure of this model.

3.1. **Model problem.** The Heston model is described by the following stock price (3.1a) and volatility (3.1b) dynamics,

$$dS = \iota S d\tau + \sigma S dW^1, \tag{3.1a}$$

$$d\nu = \kappa(\gamma - \nu)d\tau + \xi\sqrt{\nu}dW^2, \tag{3.1b}$$

The asset price $S := \{S_\tau : \tau \geq 0\}$ exhibits geometric Brownian motion with Wiener process W^1, drift ι and volatility $\sigma := \sqrt{\nu}$. The stochastic instantaneous variance $\nu := \{\nu_\tau : \tau \geq 0\}$ is driven by a mean-reverting square-root process (known as the Cox-Ingersoll-Ross (CIR) process) with long-run variance $\gamma > 0$, rate of mean reversion $\kappa > 0$, and volatility of variance (also called the volatility of volatility) $\xi > 0$. The Wiener processes W^1 and W^2 are correlated by $\rho \in [-1, 1]$. Moreover, the so-called *Feller condition* is assumed, which states that the variance process (3.1b) is strictly positive if the parameters satisfy

$$2\kappa\gamma > \xi^2, \tag{3.2}$$

see, e.g., [38]. Unless otherwise stated, we focus on setting the parameters such that the Feller condition is always fulfilled. In terms of Itô calculus, (3.1) can be reformulated as the partial differential equations (2.2), (2.3), see, e.g., [2], where $\boldsymbol{\mu} := (\xi, \rho, \gamma, \kappa, r)$, and the operator $\mathcal{L}(\boldsymbol{\mu})$ is defined as follows

$$\mathcal{L}(\boldsymbol{\mu})P(\boldsymbol{\mu}) := \frac{1}{2}\nu S^2\frac{\partial^2 P(\boldsymbol{\mu})}{\partial S^2} + \xi\nu\rho S\frac{\partial^2 P(\boldsymbol{\mu})}{\partial \nu \partial S} + \frac{1}{2}\xi^2\nu\frac{\partial^2 P(\boldsymbol{\mu})}{\partial \nu^2} + rS\frac{\partial P(\boldsymbol{\mu})}{\partial S} + \kappa(\gamma - \nu)\frac{\partial P(\boldsymbol{\mu})}{\partial \nu} - rP(\boldsymbol{\mu}). \tag{3.3}$$

We note that the operator (3.3) is of a convection-diffusion reaction type with variable coefficients that is degenerate for $S = 0$, $\nu = 0$. To eliminate the degeneracy in the asset price variable, the standard practice is to perform a log-transformation of S. Introducing the new variable $x := \log(S/K)$, we denote by $w(\tau, \nu, x, \boldsymbol{\mu}) := P(\tau, \nu, Ke^x; \boldsymbol{\mu})$ the price in the log-transformed variable, i.e., $w(0, \nu, x; \boldsymbol{\mu}) = \chi(x) := (Ke^x - K)_+$ for a put and

$\chi(x) := (K - Ke^x)_+$ for a call. Let $L(\boldsymbol{\mu})$ be the differential operator corresponding to $\mathcal{L}(\boldsymbol{\mu})$ in the log-transformed variable given by

$$L(\boldsymbol{\mu})w(\boldsymbol{\mu}) = \nabla \cdot \mathbf{A}(\boldsymbol{\mu})\nabla w(\boldsymbol{\mu}) - \mathbf{b}(\boldsymbol{\mu}) \cdot \nabla w(\boldsymbol{\mu}) - rw(\boldsymbol{\mu}), \tag{3.4a}$$

with $\nabla := \left(\frac{\partial}{\partial \nu}, \frac{\partial}{\partial x}\right)^T$, diffusion matrix $\mathbf{A}(\boldsymbol{\mu})$ and velocity vector $\mathbf{b}(\boldsymbol{\mu})$

$$\mathbf{A}(\boldsymbol{\mu}) := \frac{1}{2}\nu \begin{bmatrix} \xi^2 & \rho\xi \\ \rho\xi & 1 \end{bmatrix}, \qquad \mathbf{b}(\boldsymbol{\mu}) := \begin{bmatrix} -\kappa(\gamma - \nu) + \frac{1}{2}\xi^2 \\ -r + \frac{1}{2}\nu + \frac{1}{2}\xi\rho \end{bmatrix}. \tag{3.4b}$$

The PDE is considered on a bounded domain $\Omega := (\nu_{\min}, \nu_{\max}) \times (x_{\min}, x_{\max}) \subset \mathbb{R}^2$, $x_{\min} < 0 < x_{\max}$, $0 < \nu_{\min} < \nu_{\max}$ with the Lipschitz continuous boundary $\partial\Omega = \Gamma_{\mathrm{D}} \cup \Gamma_{\mathrm{N}}$, where Γ_{D} corresponds to the non-trivial Dirichlet part of the boundary $\partial\Omega$, and Γ_{N} stands for the Neumann part. For European put options, we consider the boundary conditions as in [20],

$$\frac{\partial w}{\partial \nu}(t, \nu, x) = 0, \qquad \text{on} \quad \Gamma_{\mathrm{N}} := \{(\nu, x) \in \Omega : \quad \nu \in \{\nu_{\min}, \nu_{\max}\}\}, \tag{3.5a}$$

$$w(t, \nu, x) = Ke^{-rt}, \qquad \text{on} \quad \Gamma_{\mathrm{D}}^1 := \{(\nu, x) \in \Omega : \quad x = x_{\min}\}, \tag{3.5b}$$

$$w(t, \nu, x) = 0, \qquad \text{on} \quad \Gamma_{\mathrm{D}}^2 := \{(\nu, x) \in \Omega : \quad x = x_{\max}\}. \tag{3.5c}$$

For American put options, we specify the boundary conditions as proposed in [15, 20],

$$w(t, \nu, x) = \chi(x), \quad \text{on} \quad \Gamma_{\mathrm{D}} := \Gamma_{\mathrm{D}}^1 \cup \Gamma_{\mathrm{D}}^2, \quad \frac{\partial w}{\partial \nu}(t, \nu, x) = 0, \quad \text{on} \quad \Gamma_{\mathrm{N}}. \tag{3.6a}$$

Next, we recast the problem in a variational form. We introduce the following functional spaces

$$X = H^1(\Omega), \quad V := \{v \in X : \ v|_{\Gamma_{\mathrm{D}}} = 0\}, \tag{3.7}$$

equipped with the norms $\|\cdot\|_X = \|\cdot\|_{H^1}$, $\|\cdot\|_V = |\cdot|_{H^1}$, which correspond to the $H^1(\Omega)$ norm and semi-norm respectively. Let V' be the dual space of V, and denote by $\langle\cdot,\cdot\rangle_{V'\times V}$ the duality pairing of V with V'. We then define the bilinear form $a : V \times V \to \mathbb{R}$ corresponding to the Heston model,

$$a(u, v; \boldsymbol{\mu}) := \int_\Omega \mathbf{A}(\boldsymbol{\mu})\nabla u \cdot \nabla v + \int_\Omega \mathbf{b}(\boldsymbol{\mu}) \cdot \nabla uv + \int_\Omega ruv. \tag{3.8}$$

Note that $\nu \geq \nu_{\min} > 0$, $\rho \in (-1, 1)$ and hence $\mathbf{A}(\boldsymbol{\mu})$ is positive definite on $\overline{\Omega}$. It follows from the admissible values of the parameters that for all $\boldsymbol{\mu} \in \mathcal{P}$ the bilinear form $a(\cdot, \cdot; \boldsymbol{\mu})$ is continuous and satisfies a Gårding inequality on $V \times V$, [51], i.e., there exist constants $0 < \overline{\alpha}_a \leq \alpha_a(\boldsymbol{\mu})$, $0 < \gamma_a(\boldsymbol{\mu}) \leq \overline{\gamma}_a < \infty$, $0 \leq \lambda_a(\boldsymbol{\mu}) \leq \overline{\lambda}_a < \infty$, such that

$$|a(u, v; \boldsymbol{\mu})| \leq \gamma_a(\boldsymbol{\mu})\|u\|_V\|v\|_V \quad \forall u, v \in V, \qquad (\textit{continuity})$$

$$a(v, v; \boldsymbol{\mu}) \geq \alpha_a(\boldsymbol{\mu})\|v\|_V^2 - \lambda_a(\boldsymbol{\mu})\|v\|_{L^2(\Omega)}^2 \quad \forall v \in V. \qquad (\textit{Gårding inequality})$$

For the semi-discretization in time, we use the θ-scheme with $\theta = 1/2$. Let $t := T - \tau$ and subdivide the time interval $[0, T]$ into I subintervals of equal length, $t^k := k\Delta t$, $0 < k \leq I$ with $\Delta t = T/I$. Defining $w^k(\boldsymbol{\mu}) := w(t^k, \nu, x; \boldsymbol{\mu}) \in X$, we decompose it into $w^k = u^k + u_L^k$, where $u^k \in V$ and $u_L^k \in X$ is a continuous extension of the inhomogeneous Dirichlet data. Furthermore, for all $\boldsymbol{\mu} \in \mathcal{P}$, $v \in V$, $\theta \in [0, 1]$, $k \in \mathbb{I}$, where $\mathbb{I} := \{0, \ldots, I - 1\}$, we define the

linear functional $f^{k+\theta}(\boldsymbol{\mu}) \in V'$ as follows

$$f^{k+\theta}(v;\boldsymbol{\mu}) := -\frac{1}{\Delta t}\left(u_L^{k+1}(\boldsymbol{\mu}) - u_L^k(\boldsymbol{\mu}), v\right)_{L^2(\Omega)} - a\left(\theta u_L^{k+1}(\boldsymbol{\mu}) + (1-\theta)u_L^k(\boldsymbol{\mu}), v;\boldsymbol{\mu}\right). \quad (3.10)$$

Using a test function $v \in V$ in (2.2) yields the following variational formulation

$$\frac{1}{\Delta t}\left(u^{k+1} - u^k, v\right)_{L^2(\Omega)} + a(u^{k+\theta}, v;\boldsymbol{\mu}) = f^{k+\theta}(v;\boldsymbol{\mu}), \quad v \in V, \quad (3.11)$$

where $u^{k+\theta} := \theta u^{k+1} + (1-\theta)u^k$.

In terms of a Lagrange multiplier, the constrained problem (2.3) can be weakly written in saddle point form, see, e.g., [39]. Define $W = V'$ and $M \subset W$ as a dual cone by

$$M := \{\eta \in W : \quad b(\eta, v) \geq 0,\ v \in V,\ v \geq 0\}, \quad (3.12)$$

where $b(\eta, v) := \langle \eta, v\rangle_{V'\times V}$, for all $\eta \in W$, $v \in V$. For $\boldsymbol{\mu} \in \mathcal{P}$ and $k \in \mathbb{I}$, we introduce the functional $g^{k+1} \in W'$,

$$g^{k+1}(\eta;\boldsymbol{\mu}) := b(\eta, \chi) - b(\eta, u_L^{k+1}(\boldsymbol{\mu})).$$

Then we arrive at the following variational saddle point formulation: For $\boldsymbol{\mu} \in \mathcal{P}$, $k \in \mathbb{I}$, $\theta \in [0,1]$, find $(u^{k+1}(\boldsymbol{\mu}), \lambda^{k+1}(\boldsymbol{\mu})) \in V \times M$, satisfying for all $\eta \in M, v \in V$,

$$\frac{1}{\Delta t}\left(u^{k+1} - u^k, v\right)_{L^2(\Omega)} + a(u^{k+\theta}, v;\boldsymbol{\mu}) - b(\lambda^{k+1}, v) = f^{k+\theta}(v;\boldsymbol{\mu}), \quad (3.13)$$

$$b(\eta - \lambda^{k+1}, u^{k+1}) \geq g^{k+1}(\eta - \lambda^{k+1};\boldsymbol{\mu}). \quad (3.14)$$

Note that for all $\boldsymbol{\mu} \in \mathcal{P}$, $k \in \mathbb{I}$, $f^{k+\theta} \in V'$ and the bilinear form $a(\cdot,\cdot;\boldsymbol{\mu})$ is continuous and satisfies the Gårding inequality. Thus, for a small enough time step $\Delta t < (1/\theta\lambda_a(\boldsymbol{\mu}))$, by a generalized Lax-Milgram argument, the problem (3.11) admits a unique solution $u(\boldsymbol{\mu}) \in V$, [2, 51]. Moreover, the bilinear from $b(\cdot,\cdot)$ is inf-sup stable on $W \times V$ and unique solvability of (3.14) is given, see, e.g., [8, Theorem 2.1].

3.2. **Calibration.** Given S_0 and the observations P_i^{obs} at (T_i, K_i), $i = 1, \ldots, M$, we need to compute the corresponding prices in the Heston model $P_i(\nu_0, S_0, T_i, K_i)$, where $\nu_0 \in \mathbb{R}_+$ is the initial volatility. However, the value of ν_0 is not observable and needs to be determined together with the parameters $\xi, \rho, \gamma, \kappa$. We collect all parameters to be identified into the single vector $\boldsymbol{\Theta} = (\Theta_1, \ldots, \Theta_5) = (\xi, \rho, \gamma, \kappa, \nu_0) \in \mathcal{P}_{\text{opt}}$, where

$$\mathcal{P}_{\text{opt}} := \left\{\boldsymbol{\Theta} \in \mathbb{R}^5 : \Theta_{\min,i} \leq \Theta_i \leq \Theta_{\max,i}, \quad i = 1, \ldots, 5\right\}. \quad (3.15)$$

We replace the PDE constraints with the corresponding weak discrete problem in a log-transformed variable. The polygonal domain $\Omega \subset \mathbb{R}^2$ is resolved by a triangulation $\mathcal{T}_\mathcal{N}$ of Ω, consisting of J simplices $T_\mathcal{N}^j$, $1 \leq j \leq J$, such that $\overline{\Omega} = \cup_{T_\mathcal{N}\in\mathcal{T}_\mathcal{N}} \overline{T}_\mathcal{N}$. We use standard conforming nodal first-order finite element approximation spaces $X_\mathcal{N} \subset X$, $V_\mathcal{N} \subset V$, where $X_\mathcal{N} := \{v \in X : \quad v_{|T_\mathcal{N}^j} \in \mathbb{P}^1(T_\mathcal{N}^j), 1 \leq j \leq J\}$, and $\mathbb{P}^1$ is a space of linear polynomials with degree at most one, and $V_\mathcal{N} = X_\mathcal{N} \cap V$, $\dim(X_\mathcal{N}) = \mathcal{N}_X$, $\dim(V_\mathcal{N}) = \mathcal{N}_V$. To discretize the dual space W, we use discontinuous piecewise linear biorthogonal basis functions defined on the same mesh as the basis functions of $V_\mathcal{N}$, [63]. That is, $W_\mathcal{N} := \text{span}\{\chi_q,\ q = 1, \ldots, \mathcal{N}\}$, $\dim(W_\mathcal{N}) = \mathcal{N}_W = \mathcal{N}_V$, where χ_q satisfy a local biorthogonality relation:

$$\int_{T_\mathcal{N}^j} \chi_q \phi_p = \delta_{pq} \int_{T_\mathcal{N}^j} \phi_p \geq 0, \quad \phi_p \in V_\mathcal{N}, \quad p, q = 1, \ldots, \mathcal{N}_V.$$

The discrete cone $M_{\mathcal{N}} \subset W_{\mathcal{N}}$ is given as

$$M_{\mathcal{N}} = \operatorname{span}_+\{\chi_q\}_{q=1}^{\mathcal{N}_W} := \Big\{\eta \in W_{\mathcal{N}} : \quad \eta = \sum_{q=1}^{\mathcal{N}_W} \alpha_q \chi_q, \quad \alpha_q \geq 0\Big\} \tag{3.16}$$

and $(V_{\mathcal{N}}, W_{\mathcal{N}})$ form a uniformly inf-sup stable pairing.

For a given $\boldsymbol{\mu} \in \mathcal{P}$, $k \in \mathbb{I}$, we approximate $w^k(\boldsymbol{\mu})$ by $w^k_{\mathcal{N}}(\boldsymbol{\mu}) \in X_{\mathcal{N}}$, $w^k_{\mathcal{N}}(\boldsymbol{\mu}) := u^k_{\mathcal{N}}(\boldsymbol{\mu}) + u^k_{L\mathcal{N}}(\boldsymbol{\mu})$ with $u^k_{\mathcal{N}}(\boldsymbol{\mu}) \in V_{\mathcal{N}}$ and $u^k_{L\mathcal{N}}(\boldsymbol{\mu}) \in X_{\mathcal{N}}$ and $\lambda^{k+1}(\boldsymbol{\mu})$ by $\lambda^{k+1}_{\mathcal{N}}(\boldsymbol{\mu}) \in M_{\mathcal{N}}$, $k \in \mathbb{I}$. In the reduced basis literature it is common to call $u^k_{\mathcal{N}}(\boldsymbol{\mu})$ and $\lambda^k_{\mathcal{N}}(\boldsymbol{\mu})$ the detailed solutions.

Then, for the European put options $u^{k+1}_{\mathcal{N}}(\boldsymbol{\mu}) \in V_{\mathcal{N}}$, $\boldsymbol{\mu} \in \mathcal{P}$, $k \in \mathbb{I}$, solves the following discrete problem

$$\mathbb{E}^{\mathrm{Eu}}_{\mathcal{N}}(\boldsymbol{\mu}) = \begin{cases} \frac{1}{\Delta t}\left(u^{k+1}_{\mathcal{N}} - u^k_{\mathcal{N}}, v\right)_{L^2(\Omega)} + a(u^{k+\theta}_{\mathcal{N}}, v; \boldsymbol{\mu}) = f^{k+\theta}(v; \boldsymbol{\mu}), \\ (u^0_{\mathcal{N}} - u^0, v)_V = 0, \qquad v \in V_{\mathcal{N}}. \end{cases}$$

The solution pair $(u^{k+1}_{\mathcal{N}}(\boldsymbol{\mu}), \lambda^{k+1}_{\mathcal{N}}(\boldsymbol{\mu})) \in V_{\mathcal{N}} \times M_{\mathcal{N}}$, $\boldsymbol{\mu} \in \mathcal{P}$, $k \in \mathbb{I}$, for the American option problem in turn satisfies the following detailed saddle point problem

$$\mathbb{E}^{\mathrm{Am}}_{\mathcal{N}}(\boldsymbol{\mu}) = \begin{cases} \frac{1}{\Delta t}\left(u^{k+1}_{\mathcal{N}} - u^k_{\mathcal{N}}, v\right)_{L^2(\Omega)} + a(u^{k+\theta}_{\mathcal{N}}, v; \boldsymbol{\mu}) - b(\lambda^{k+1}_{\mathcal{N}}, v) = f^{k+\theta}(v; \boldsymbol{\mu}), \\ b(\eta - \lambda^{k+1}_{\mathcal{N}}, u^{k+1}_{\mathcal{N}}) \geq g^{k+1}(\eta - \lambda^{k+1}_{\mathcal{N}}; \boldsymbol{\mu}), \qquad \eta \in M_{\mathcal{N}}, v \in V_{\mathcal{N}}, \\ (u^0_{\mathcal{N}} - u^0, v)_V = 0. \end{cases}$$

Both problems have a unique discrete solution, and for $i = 1, \ldots, M$ we denote the approximate model price as

$$P_i^{\mathcal{N},\mathrm{s}}(\boldsymbol{\Theta}) := w^{k_i}_{\mathcal{N}}(\log(S_0/K_i), \nu_0; \boldsymbol{\mu}),$$

which is obtained from the solutions of $\mathbb{E}^s_{\mathcal{N}}$, $s \in \{\mathrm{Eu}, \mathrm{Am}\}$. By abuse of notation, we often omit the index s in the notation of $P_i^{\mathcal{N},s}$, if it is clear from context. Then the minimization problem (2.1) can be written in the following form

$$\min_{\boldsymbol{\Theta} \in \mathcal{P}_{\mathrm{opt}}} J_{\mathcal{N}}(\boldsymbol{\Theta}) := \frac{1}{M} \sum_{i=1}^{M} |P_i^{\mathrm{obs}} - P_i^{\mathcal{N}}(\boldsymbol{\Theta})|^2. \tag{3.17}$$

4. Reduced basis method (RBM)

The high-fidelity discrete problem $\mathbb{E}_{\mathcal{N}}$, in general, is computationally expensive for large $\mathcal{N}_V$, and significantly slows down the calibration procedure. To reduce the complexity, we apply the reduced basis method and substitute the detailed model $\mathbb{E}_{\mathcal{N}}$ with the reduced-order surrogate model $\mathbb{E}_N$. Using a suitable basis generation procedure, as discussed below, we construct the low-dimensional reduced spaces $V_N \subset V_{\mathcal{N}}$ for European options and $V_N \subset V_{\mathcal{N}}$, $W_N \subset W_{\mathcal{N}}$, $M_N \subset M_{\mathcal{N}}$ for American options with $\dim(V_N) \ll \dim(V_{\mathcal{N}})$, $\dim(W_N) \ll \dim(W_{\mathcal{N}})$. For a given $\boldsymbol{\mu} \in \mathcal{P}$, we approximate $u^{k+1}_{\mathcal{N}} \in V_{\mathcal{N}}$ by $u^{k+1}_N(\boldsymbol{\mu}) \in V_N$, $\lambda^{k+1}_{\mathcal{N}}(\boldsymbol{\mu}) \in M_{\mathcal{N}}$ by $\lambda^{k+1}_N(\boldsymbol{\mu}) \in M_N$, $k \in \mathbb{I}$. The reduced surrogate models for pricing

European and American options are defined as follows

$$\mathbb{E}_N^{\mathrm{Eu}}(\boldsymbol{\mu}) = \begin{cases} \frac{1}{\Delta t}\left(u_N^{k+1} - u_N^k, v\right)_{L^2(\Omega)} + a(u_N^{k+\theta}, v; \boldsymbol{\mu}) = f^{k+\theta}(v; \boldsymbol{\mu}), \\ (u_N^0 - u_{\mathcal{N}}^0, v)_V = 0, \qquad v \in V_N. \end{cases}$$

$$\mathbb{E}_N^{\mathrm{Am}}(\boldsymbol{\mu}) = \begin{cases} \frac{1}{\Delta t}\left(u_N^{k+1} - u_N^k, v\right)_{L^2(\Omega)} + a(u_N^{k+\theta}, v; \boldsymbol{\mu}) - b(\lambda_N^{k+1}, v) = f^{k+\theta}(v; \boldsymbol{\mu}), \\ b(\eta - \lambda_N^{k+1}, u_N^{k+1}) \geq g^{k+1}(\eta - \lambda_N^{k+1}; \boldsymbol{\mu}), \qquad \eta \in M_N,\ v \in V_N, \\ (u_N^0 - u_{\mathcal{N}}^0, v)_V = 0. \end{cases}$$

Additionally, we require that the reduced spaces V_N, W_N are constructed such that the bilinear form $b(\cdot,\cdot)$ is uniformly inf-sup stable on $W_N \times V_N$ with respect to N. Thus the well-posedness of the reduced problems $E_N^{\mathrm{Eu}}(\boldsymbol{\mu})$ and $E_N^{\mathrm{Am}}(\boldsymbol{\mu})$ is given, see also [12, 31].

We denote the reduced basis approximation of the model price by

$$P_i^{N,s}(\boldsymbol{\Theta}) := w_N^{k_i}(\log(S_0/K_i), \nu_0; \boldsymbol{\mu}),$$

where $w_N^{k_i}(\boldsymbol{\mu}) := u_N^{k_i}(\boldsymbol{\mu}) + u_{L\mathcal{N}}^{k_i}(\boldsymbol{\mu})$ and $u_N^{k_i}(\boldsymbol{\mu})$ is a solution of $\mathbb{E}_{\mathcal{N}} := \mathbb{E}_{\mathcal{N}}^s$, $s = \{\mathrm{Eu}, \mathrm{Am}\}$ for $i = 1, \ldots, M$. Then we approximate $J_{\mathcal{N}}(\boldsymbol{\Theta}) \approx J_N(\boldsymbol{\Theta})$, and obtain the following minimization problem for the reduced model

$$\min_{\boldsymbol{\Theta} \in \mathcal{P}_{\mathrm{opt}}} J_N(\boldsymbol{\Theta}) := \frac{1}{M} \sum_{i=1}^{M} |P_i^{\mathrm{obs}} - P_i^N(\boldsymbol{\Theta})|^2. \tag{4.1}$$

Remark 4.1. *Note that the interest rate r is not determined by a calibration procedure and is fixed beforehand. In our case, the market data will be a single stock in the U.S., and for an approximation of the risk-free rate we use the rates of the U.S. Department of the Treasury. Hence, to construct the reduced basis spaces, we only need to consider the variation of four parameters $\boldsymbol{\mu} = (\xi, \rho, \gamma, \kappa) \in \mathcal{P} \subset \mathbb{R}^4$. However, this choice is restrictive and for new market data we would need to construct a new reduced basis set. Therefore, to conserve generality in our approach, we consider the variation of all parameters, $\boldsymbol{\mu} = (\xi, \rho, \gamma, \kappa, r)$, and consequently the constructed reduced basis will be entirely market-independent.*

Numerous approaches exist for the construction of the reduced basis approximation spaces. Their common goal is to exploit the parameter dependence of the problem and to incorporate this information into the construction of the reduced bases. Typically, this is done by applying an iterative greedy strategy to a set of snapshots, i.e., solutions computed for different parameter values. For linear parabolic problems, a popular choice is a combination of the greedy strategy for parameter selection and a proper orthogonal decomposition (POD) in time resulting in a so-called POD-Greedy algorithm [28, 30]. For parabolic variational inequalities, the construction is more challenging due to the requirement of uniform inf-sup stability. For stationary variational inequalities, a greedy sampling is commonly used, [31, 64], while for time-dependent problems a POD-Angle-Greedy [12] and a POD-NNMF[1] [4] have been considered in the literature. In the present work, we follow the idea of the POD-Greedy algorithm for European options and POD-Angle-Greedy algorithm for American options.

Since the European option problem can be considered as a particular case of the American option problem formulation, we focus on the description of the basis construction for the latter problem and comment only on the differences.

[1]NNMF refers to a non-negative matrix factorization procedure, [40].

Consider a finite subset $\mathcal{P}_N := \{\boldsymbol{\mu}_1, \ldots, \boldsymbol{\mu}_N\}$, $\boldsymbol{\mu}_i \neq \boldsymbol{\mu}_j$, $\forall i \neq j$, $N \in \mathbb{N}$ and define the reduced spaces $V_N := \operatorname{span}\{\Psi_N\}$ and $W_N := \operatorname{span}\{\Xi_N\}$, where the primal $\Psi_N := \{\psi_1, \ldots, \psi_{N_V}\} \subset V_{\mathcal{N}}$, and the dual $\Xi_N := \{\xi_1, \ldots, \xi_{N_W}\} \subset W_{\mathcal{N}}$ reduced bases are constructed from the large set of snapshot solutions $u^k_{\mathcal{N}}(\boldsymbol{\mu}_i)$ and $\lambda^{k+1}_{\mathcal{N}}(\boldsymbol{\mu}_i)$, $k \in \mathbb{I}$, $i = 1, \ldots, N$. The reduced cone is defined as $M_N := \operatorname{span}_+\{\xi_j\}_{j=1}^{N_W} := \left\{\sum_{j=1}^{N_W} \alpha_j \xi_j,\ \alpha_j \geq 0\right\}$. By construction $\xi_j \in M_{\mathcal{N}}$ and thus $M_N \subset M_{\mathcal{N}}$.

The approach we follow to construct Ψ_N and Ξ_N is presented in Algorithm 1. We investigate the parameter domain $\mathcal{P}$, that is replaced by a finite set $\mathcal{P}_{\text{train}} \subset \mathcal{P}$, by a greedy search (Step 5–Step 13). In the greedy loop, we identify a "worst" parameter $\boldsymbol{\mu}_N$, i.e., a parameter which leads to the worst RB approximation, and add it to the training set. This selection requires an error measure $E_N(\boldsymbol{\mu}_N)$, which can be chosen, e.g., as the true error between the detailed solution and the reduced basis approximation or an a posteriori error bound [12, 27, 30]. The availability and efficient computation of the latter choice makes it more attractive from a computational point of view. Next, for the selected parameter, we compute primal and dual bases and repeat this process $N_{\max}$ times or until the desired tolerance ε_{tol} of the stopping criterion is reached. For the primal reduced space construction, we apply the standard POD-Greedy procedure (Step 11), where the difference between the worst resolved trajectory $u^k_{\mathcal{N}}(\boldsymbol{\mu}_N)$, $k \in \mathbb{I}$, and its orthogonal projection onto the current RB space $\Pi_{V_{N-1}} u^k_{\mathcal{N}}(\boldsymbol{\mu}_N)$ is compressed to the first dominant POD mode:

$$POD_1\left(\{v^k\}_{k\in\mathbb{I}_0}\right) := \underset{\|z\|_V=1}{\arg\min} \sum_{k\in\mathbb{I}_0} \|v^k - (v^k, z)_V z\|_V^2.$$

Algorithm 1 POD-Angle-Greedy Algorithm

Input: Maximum number of iterations $N_{\max} > 0$, training sample set $\mathcal{P}_{\text{train}} \subset \mathcal{P}$, target tolerance ε_{tol}

Output: RB bases Ψ_N, Ξ_N and RB spaces V_N, W_N

1: arbitrarily choose $\boldsymbol{\mu}_0 \in \mathcal{P}_{\text{train}}$ and $k' \in \mathbb{I}_0 := \mathbb{I} \cup \{I\}$
2: compute $\{u^k_{\mathcal{N}}(\boldsymbol{\mu}_0)\}_{k\in\mathbb{I}_0}$, $\{\lambda^{k+1}_{\mathcal{N}}(\boldsymbol{\mu})\}_{k\in\mathbb{I}}$
3: set $\xi_0 = \lambda^{k'}_{\mathcal{N}}(\boldsymbol{\mu}_0)/\|\lambda^{k'}_{\mathcal{N}}(\boldsymbol{\mu}_0)\|_W$, $\Xi_0 = \{\xi_0\}$, $W_0 = \operatorname{span}\{\Xi_0\}$
4: set $\Psi_0 = \text{orthonormalize}\left\{u^{k'}_{\mathcal{N}}(\boldsymbol{\mu}_0), T\xi_0\right\}$, $V_0 = \operatorname{span}\{\Psi_0\}$
5: **for** $N = 1, \ldots, N_{\max}$ **do**
6: $\quad\boldsymbol{\mu}_N = \arg\max_{\boldsymbol{\mu}\in\mathcal{P}_{\text{train}}} E_{N-1}(\boldsymbol{\mu})$
7: $\quad$**if** $\varepsilon_N^{\text{train}} < \varepsilon_{\text{tol}}$ **then return**
8: $\quad$**end if**
9: $\quad k_N = \arg\max_{k\in\mathbb{I}} \left(\measuredangle\left(\lambda^{k+1}_{\mathcal{N}}(\boldsymbol{\mu}_N), W_{N-1}\right)\right)$
10: $\quad\xi_N = \lambda^{k_N}_{\mathcal{N}}(\boldsymbol{\mu}_N)/\|\lambda^{k_N}_{\mathcal{N}}(\boldsymbol{\mu}_N)\|_W$, $\Xi_N = \Xi_{N-1} \cup \{\xi_N\}$, $W_N = \operatorname{span}\{\Xi_N\}$
11: $\quad\psi_N = POD_1\left(\left\{u^k_{\mathcal{N}}(\boldsymbol{\mu}_N) - \Pi_{V_{N-1}}\left(u^k_{\mathcal{N}}(\boldsymbol{\mu}_N)\right)\right\}_{k\in\mathbb{I}_0}\right)$
12: $\quad\Psi_N = \text{orthonormalize}\{\Psi_{N-1} \cup \{\psi_N, T\xi_N\}\}$, $V_N = \operatorname{span}\{\Psi_N\}$
13: **end for**

To construct the dual RB space, the vectors that maximize the volume of the resulting cone, i.e., vectors showing the largest deviation from the current RB space (Step 9, are selected. We denote $\measuredangle(\eta, Y) := \arccos\left(\|\Pi_Y \eta\|_W / \|\eta\|_W\right)$ the angle between the vector $\eta \in W$ and the linear space $Y \subset W$, where $\Pi_Y \eta$ is an orthogonal projection of η onto Y.

Additionally, to form a uniformly stable pair of the reduced spaces V_N, W_N, we enrich the primal space V_N by the "supremizing" $T\xi_N$, [53, 54], where $T : W_{\mathcal{N}} \to V_{\mathcal{N}}$ is a "supremizing" operator, defined as a solution of $(T\xi_N, v)_V := b(\xi_N, v)$, for all $v \in V_{\mathcal{N}}$. It is easy to see that this inclusion ensures the inf-sup stability of $b(\cdot,\cdot)$ on $W_N \times V_N$, see, e.g., [31, 54, 31].

For the case of European options no dual space is required and thus the steps in Algorithm 1 involving the Lagrange multiplier space are omitted, resulting in a standard POD-Greedy algorithm.

A computational speed-up of this method is achieved by a so-called offline/online procedure, which relies on the assumption that the problem has an affine dependence on its parameters. That is, for every $\boldsymbol{\mu} \in \mathcal{P}$ the bilinear and linear forms are separable, i.e., there exist $\Theta_q^a : \mathcal{P} \to \mathbb{R}$, $q = 1, \dots, Q_a$, such that $a(\cdot,\cdot;\boldsymbol{\mu}) := \sum_{q=1}^{Q_a} \Theta_q^a(\boldsymbol{\mu}) a_q(\cdot,\cdot)$, where $a_q : V \times V \to \mathbb{R}$ are parameter-independent. The same arguments apply to $f^{k+\theta}(\cdot;\boldsymbol{\mu})$, $g^k(\cdot;\boldsymbol{\mu})$ and $u_{\mathcal{N}}^0(\boldsymbol{\mu})$. Then an offline routine requires the evaluation of all parameter-independent quantities. Usually this procedure is computationally cost-intense, however it is performed only once. In turn, the online procedure is computationally cheap and involves assembling the parameter-dependent components and solving the reduced system. This stage is executed multiple times for each new parameter value $\boldsymbol{\mu} \in \mathcal{P}$; see, e.g., [32, 50] for more details.

5. De-Americanization strategy (DAS)

In contrast to the reduced basis framework, which is based on the underlying pricing PDE, the DAS transforms the observed American market prices into pseudo-European prices prior to the calibration. That is, given an input data of American put options, we consider the minimization problem (3.17) with $J_{\mathcal{N}}(\boldsymbol{\Theta}) \approx \widetilde{J}_{\mathcal{N}}(\boldsymbol{\Theta})$,

$$\min_{\boldsymbol{\Theta} \in \mathcal{P}_{\text{opt}}} \widetilde{J}_{\mathcal{N}}(\boldsymbol{\Theta}) := \frac{1}{M} \sum_{i=1}^{M} |\widetilde{P}_i^{\text{obs}} - P_i^{\mathcal{N}}(\boldsymbol{\Theta})|^2, \tag{5.1}$$

where the prices $\widetilde{P}_j^{\text{obs}}$ are the pseudo-European put prices. These are obtained by perturbing the American put prices P_j^{obs}, i.e., $\widetilde{P}_j^{\text{obs}} := D(P_j^{\text{obs}})$, where $D : \mathbb{R}^M \to \mathbb{R}^M$, and the corresponding model prices are the European put prices, $P_j^{\mathcal{N}}(\boldsymbol{\Theta}) = P_j^{\mathcal{N},\text{Eu}}(\boldsymbol{\Theta})$. As in [11], we use the binomial tree method, see [18], to transform American option prices into pseudo-European option prices. In a nutshell, once the observed market prices $P_j^{\text{obs}}, j = 1, \dots, M$, have been collected, for each single stock option an individual binomial tree is calibrated to match this option price P_j^{obs}. The resulting tree is used to price the associated so-called pseudo-European option with the same strike and maturity. A detailed description of the de-Americanization method is given in [11, Algorithm 1].

The advantage of this method is that the complexity of the non-linear model for pricing American options can be reduced to that of the linear model for pricing European options, allowing closed-form solutions or Fourier techniques to be exploited.

In the following, we denote the prices obtained by the semi-closed-form solutions by P_i^{CF}, see [33]. This leads to the following minimization problem

$$\min_{\boldsymbol{\Theta} \in \mathcal{P}_{\text{opt}}} \widetilde{J}_{\text{CF}}(\boldsymbol{\Theta}) := \frac{1}{M} \sum_{i=1}^{M} |\widetilde{P}_i^{\text{obs}} - P_i^{\text{CF}}(\boldsymbol{\Theta})|^2. \tag{5.2}$$

We note that from the computational point of view, the DAS is very attractive, particularly in combination with the closed-form solutions. However, for each set of observations,

an additional pre-processing time to transform the American data into European one is required, and, as we will see later, this step can dominate the computational cost of the entire calibration routine.

One could also consider a combination of the RBM with the de-Americanization strategy, i.e., applying the RBM to approximate E_N^{Eu} by E_N^{Eu}. The corresponding minimization problem can be stated as follows

$$\min_{\boldsymbol{\Theta}\in\mathcal{P}_{\mathrm{opt}}} \widetilde{J}_N(\boldsymbol{\Theta}) := \frac{1}{M}\sum_{i=1}^{M} |\widetilde{P}_i^{\mathrm{obs}} - P_i^N(\boldsymbol{\Theta})|^2, \tag{5.3}$$

with $P_i^N(\boldsymbol{\Theta}) = P_i^{N,\mathrm{Eu}}(\boldsymbol{\Theta})$. We note that due to the presence of the box constraints this finite-dimensional minimization problem admits a solution, see, e.g., [62].

6. Numerical results

The problems under consideration belong to the class of finite-dimensional optimization problems with box constraints and thus suitable numerical algorithms have to be applied. For the special case of the calibration with European options, the most popular optimization algorithms are the gradient-based optimization methods; see, e.g., [2, 56] and the references therein. By contrast, for American options, the situation is more involved due to non-differentiability, see, e.g., [37, 35, 60]. Here, we use the MATLAB Optimization Toolbox and apply the built-in "black-box" optimization solver *lsqnonlin* or *fmincon*, in which the gradients are approximated by finite differences.

For the numerical experiments we set $T = 2$, $I = 250$, $\Delta t = T/I = 0.008$, $\theta = 1/2$. The computational domain $\Omega = (\nu_{\min}, \nu_{\max}) \times (x_{\min}, x_{\max}) = (10^{-5}, 3) \times (-5, 5)$ is resolved by a triangulation with $\mathcal{N}_X = 4753$ nodes. For $\boldsymbol{\mu} := (\xi, \rho, \gamma, \kappa, r) \in \mathcal{P} \subset \mathbb{R}^5$ and $\boldsymbol{\Theta} := (\xi, \rho, \gamma, \kappa, \nu_0) \in \mathcal{P}^{\mathrm{opt}} \subset \mathbb{R}^5$, we define

$$\mathcal{P} \equiv [0.1, 0.9] \times [-0.95, 0.95] \times [0.01, 0.5] \times [0.1, 5] \times [0.0001, 0.8], \tag{6.1}$$

$$\mathcal{P}^{\mathrm{opt}} \equiv [0.1, 0.9] \times [-0.95, 0.3] \times [0.01, 0.5] \times [0.1, 5] \times [10^{-5}, 1]. \tag{6.2}$$

Unless otherwise stated, the calibration routine is performed with with *lsqnonlin*, which uses a Trust-Region-Reflective algorithm, and the stopping criterion is set as $J(\boldsymbol{\Theta}) - J(\boldsymbol{\Theta}^\star) \leq 10^{-12}$, $\|\boldsymbol{\Theta} - \boldsymbol{\Theta}^\star\|_2 \leq 10^{-5}$, where $\boldsymbol{\Theta}^\star$ is a locally optimal solution.

6.1. Calibration based on RBM.

We consider a training set $\mathcal{P}_{\mathrm{train}}$ composed of uniformly distributed points in $\mathcal{P}$ with $|\mathcal{P}_{\mathrm{train}}| = 1024$ for the European put and $|\mathcal{P}_{\mathrm{train}}| = 3125$ for the American put options. The bases are generated by the POD-Greedy and POD-Angle-Greedy algorithms for the European and the American options, respectively. The reduced systems have dimension $N_{\max} = 100$ for European put and $N_{\max} = 125$ for American put options. Firstly, we consider the quality of the calibration in terms of the RBM applied to a synthetic data set with $r = 5\%$:

$$
\begin{aligned}
&S_0 = 1, \\
&T_1 = \frac{1}{6}, \qquad && K_1 = \{0.95, 0.975, 1, 1.025, 1.05\}, \\
&T_2 = \frac{1}{2}, \qquad && K_2 = K_1 \cup \{0.9, 0.925, 1.075, 1.1\}, \\
&T_3 = \frac{3}{4}, \qquad && K_3 = K_2 \cup \{0.85, 0.875, 1.125, 1.15\}, \\
&T_4 = 1, \qquad && K_4 = K_3 \cup \{0.8, 0.825, 1.175, 1.2\}, \\
&T_5 = 2, \qquad && K_5 = K_4 \cup \{0.75, 0.775, 1.225, 1.25\}.
\end{aligned} \tag{6.3}
$$

For each pair $(T_i, K_i)_{i=1,\dots,5}$, we generate two artificial sets of observations P^{obs} consisting of 65 European and American put options at $\boldsymbol{\Theta} = (0.7, -0.8, 0.3, 1.4, 0.3)$. That is, we solve the detailed problems (3.17) with $\mathbb{E}^{\text{Am}}_{\mathcal{N}}$ and $\mathbb{E}^{\text{Eu}}_{\mathcal{N}}$ for the parameter $\boldsymbol{\mu} = (0.7, -0.8, 0.3, 1.4, 0.05)$ and $K = 1$ and interpolate the corresponding solution $K_i u^{k_i}_{\mathcal{N}}(\nu, x; \boldsymbol{\mu})$ at $\nu^\star = \nu_0$, $x_i^\star = \log(S_0/K_i)$.

We perform the optimization routine with the reduced surrogate model (4.1) and the high-fidelity detailed problem (3.17). In both cases, we use the same initial guess $\boldsymbol{\Theta}_{\text{in}}$ for the optimization algorithm. The results of the calibration for two different data sets of American and European options are presented in Table 1. We observe that, using the detailed models $\mathbb{E}^s_{\mathcal{N}}$, $\{s = \text{Am}, \text{Eu}\}$, we can basically recover the exact parameters $\boldsymbol{\Theta}_{\text{ex}}$. The reduced surrogate models provide still accurate enough results but are computationally much less expensive.

Method	$\mathbb{E}(\boldsymbol{\mu})$	$\boldsymbol{\Theta}$	ξ	ρ	γ	κ	ν_0	$\|\boldsymbol{\Theta}_{\text{ex}} - \boldsymbol{\Theta}^\star\|_2$
		$\boldsymbol{\Theta}_{\text{ex}}$	0.700	-0.800	0.300	1.400	0.300	
		$\boldsymbol{\Theta}_{\text{in}}$	0.601	-0.682	0.487	2.020	0.496	
$J_{\mathcal{N}}(\boldsymbol{\Theta})$	$\mathbb{E}^{\text{Am}}_{\mathcal{N}}$	$\boldsymbol{\Theta}^\star$	0.700	-0.800	0.300	1.399	0.300	2.14e-5
$J_N(\boldsymbol{\Theta})$	$\mathbb{E}^{\text{Am}}_N$	$\boldsymbol{\Theta}^\star$	0.694	-0.831	0.298	1.447	0.303	5.62e-2
$J_{\mathcal{N}}(\boldsymbol{\Theta})$	$\mathbb{E}^{\text{Eu}}_{\mathcal{N}}$	$\boldsymbol{\Theta}^\star$	0.700	-0.800	0.300	1.399	0.300	2.05e-5
$J_N(\boldsymbol{\Theta})$	$\mathbb{E}^{\text{Eu}}_N$	$\boldsymbol{\Theta}^\star$	0.616	-0.886	0.293	1.306	0.300	1.52e-1

TABLE 1. Calibration of the synthetic data set of American and European put options in the Heston model using detailed and reduced problems.

The influence of the calibration process on the accuracy of the option price for different strike and maturity values are shown in Figure 1 for both American and European options. In all plots, we hardly observe any differences in the option price obtained from the synthetic and the calibrated data with the detailed problem and the reduced problem.

The run-time performance is reported in Table 2. Additionally, we state the number of required iteration steps in the optimization algorithm and the number of function calls.

In this example, the optimization routine with the surrogate reduced model is about 100 times faster for American put options and about 350 times faster for European put options. The reduced model for American options recovers the parameter slightly better than the European one. This fact can be explained by the larger dimension of the reduced system for American options and the larger training set, which is also reflected in the run-time performance. We point out, that depending on the priority of the task, i.e., accuracy vs. the run-time, one can always manually adjust the dimension of the reduced system.

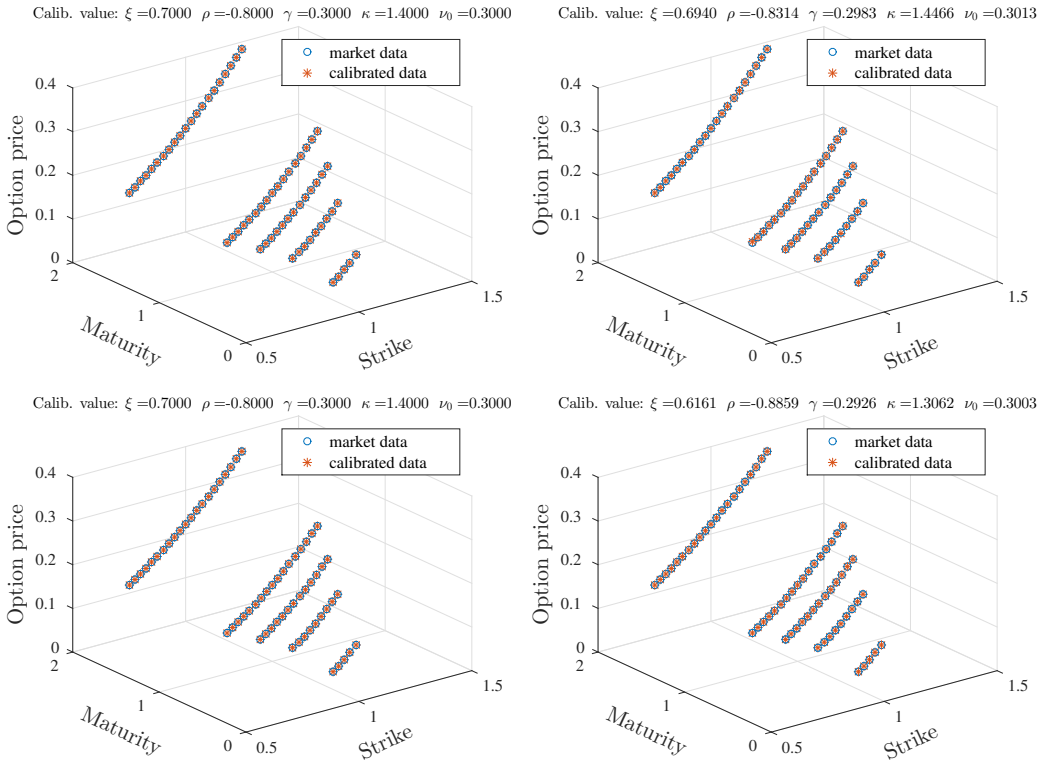

FIGURE 1. Results of the calibration to the synthetic data set of American (upper row) and European (lower row) put options in the Heston model using the detailed model $\mathbb{E}_{\mathcal{N}}(\boldsymbol{\mu})$ (left) and the reduced surrogate model $\mathbb{E}_{N}(\boldsymbol{\mu})$ (right). The circles are the synthetic prices and the stars are the prices in the calibrated model.

Method	$\mathbb{E}(\boldsymbol{\mu})$	# iter.	# J	calib. time	$J(\boldsymbol{\Theta}^\star)$
$J_{\mathcal{N}}(\boldsymbol{\Theta})$	$\mathbb{E}_{\mathcal{N}}^{\mathrm{Am}}$	7	48	15.59 hrs	1.698e-16
$J_{N}(\boldsymbol{\Theta})$	$\mathbb{E}_{N}^{\mathrm{Am}}$	8	54	9.50 min	9.515e-9
$J_{\mathcal{N}}(\boldsymbol{\Theta})$	$\mathbb{E}_{\mathcal{N}}^{\mathrm{Eu}}$	7	48	11.67 hrs	1.242e-16
$J_{N}(\boldsymbol{\Theta})$	$\mathbb{E}_{N}^{\mathrm{Eu}}$	11	72	1.996 min	1.157e-08

TABLE 2. Calibration results for the synthetic data set of American and European put options in the Heston model in terms of the run-time performance. The number "# iter." corresponds to the number of iterations and "# J" is the total number of function evaluations performed by the optimization routine.

To quantify the differences between reduced and detailed calibration, we plot the pointwise relative errors $|P_i^{\mathrm{obs}} - P_i^s(\boldsymbol{\Theta}^\star)|/P_i^{\mathrm{obs}}$, $s = \{\mathcal{N}, N\}$, $i = 1, \ldots, M$ in Figure 2. We observe that the reduced models yield a very good fit to the synthetic data with relative errors within the 0.5%-margin.

6.2. **Influence of the DAS on option pricing.** To study the effects of the DAS, we consider the difference between the de-Americanized put option prices and the corresponding

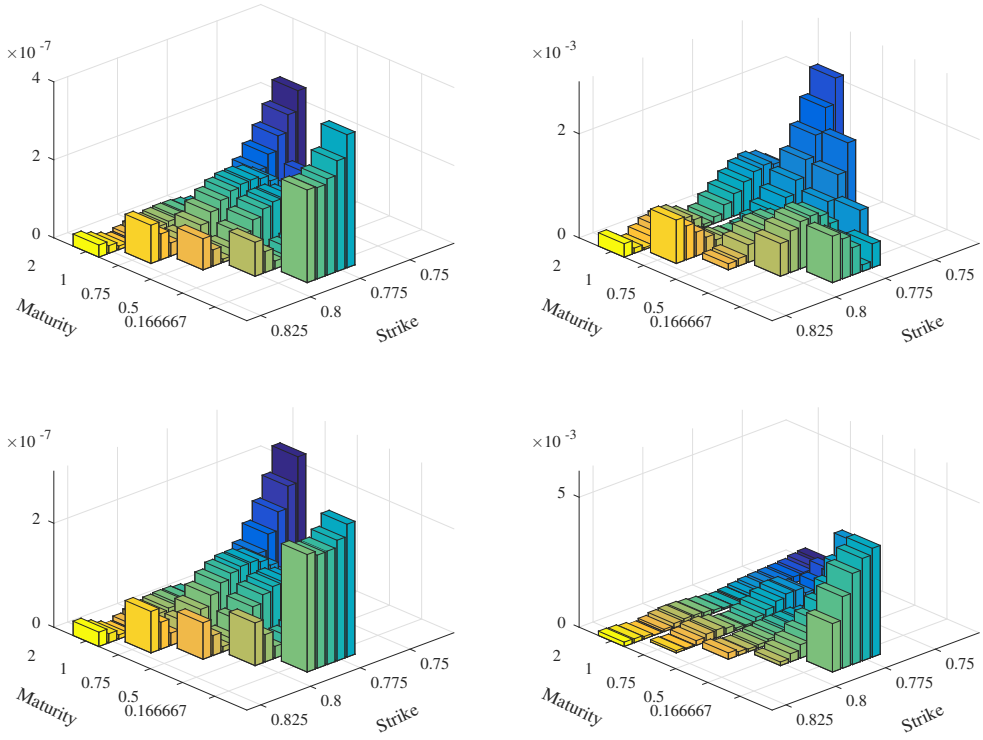

FIGURE 2. Calibration results for the synthetic data set of American (upper row) and European (lower row) put options in terms of point-wise absolute relative errors, $|P_i^{\text{obs}} - P_i^{s,\text{Am}}(\boldsymbol{\Theta}^\star)|/P_i^{\text{obs}}$, $i = 1, \ldots, M$, using the Heston model. Left: calibration with the detailed model $\mathbb{E}_{\mathcal{N}}(\boldsymbol{\mu})$, $s = \mathcal{N}$. Right: calibration with the reduced surrogate model $\mathbb{E}_N(\boldsymbol{\mu})$, $s = N$.

European ones. We set $S_0 = 1$, $r = 5\%$,

$$K = \{0.80, 0.85, 0.90, 0.95, 1.00, 1.05, 1.10, 1.15, 1.20\}$$
$$T = \left\{ \frac{1}{12}, \frac{2}{12}, \frac{3}{12}, \frac{4}{12}, \frac{6}{12}, \frac{9}{12}, \frac{12}{12}, \frac{24}{12} \right\}$$

and consider five different parameter sets, presented in Table 3. The leverage effect, that is, negative correlation between stocks and their volatilities, is commonly observed in statistical tests. This effect was cited as one of the motivating reasons for introducing local volatility models, see [17]. In our study, we therefore consider only negative values of the correlation parameter ρ. We note that in some economical studies, e.g., [23], it was shown that the negative correlations between stocks and their volatilities sometimes are not primarily connected to the actual leverage, i.e., capital structure of a company, but to the general behavior in periods when the market is in downward movement.

Starting from scenario p_1, we increase both the volatility of volatility parameter ξ and the correlation ρ, and accordingly increase the long-run variance γ and the mean reversion speed κ. In all scenarios, the initial volatility is set to the value of the mean reversion γ, i.e., $\nu_0 = \gamma$. Using these settings, we simulate the respective American put option prices in the Heston model, $P_i^{\mathcal{N},\text{Am}}$, $i = 1, \ldots, 72$. Then, applying the de-Americanized approach, we translate these option prices into the corresponding European put options

Scenario	ξ	ρ	γ	κ	ν_0
p_1	0.10	-0.20	0.07	0.1	0.07
p_2	0.25	-0.50	0.10	0.4	0.10
p_3	0.40	-0.50	0.15	0.6	0.15
p_4	0.55	-0.45	0.20	1.2	0.20
p_5	0.70	-0.80	0.30	1.4	0.30

TABLE 3. Overview of the parameter sets to study the DAS effect

$\widetilde{P}_i^{\mathcal{N},\mathrm{Eu}} := D(P_i^{\mathcal{N},\mathrm{Am}})$. To investigate the error produced by this transformation, we compare the European put options produced by the de-Americanization method $\widetilde{P}_i^{\mathcal{N},\mathrm{Eu}}$ with the European put options obtained by solving the Heston PDE directly, $P_i^{\mathcal{N},\mathrm{Eu}}$. The values of the maximal error ($\max_i |\widetilde{P}_i^{\mathcal{N},\mathrm{Eu}}(\boldsymbol{\Theta}) - P_i^{\mathcal{N},\mathrm{Eu}}(\boldsymbol{\Theta})|$) are presented in Table 4. The reference values ($\max_i P_i^{\mathcal{N},\mathrm{Eu}}(\boldsymbol{\Theta})$) are presented in the third column.

	Maximal absolute difference								Maximal European price							
	T_1	T_2	T_3	T_4	T_5	T_6	T_7	T_8	T_1	T_2	T_3	T_4	T_5	T_6	T_7	T_8
p_1	5e-4	2e-3	2e-4	1e-4	2e-4	2e-4	9e-5	3e-4	0.195	0.193	0.191	0.191	0.192	0.194	0.195	0.198
p_2	8e-4	6e-5	3e-4	9e-5	2e-5	2e-5	7e-5	4e-4	0.196	0.195	0.195	0.197	0.200	0.204	0.208	0.217
p_3	2e-4	1e-4	1e-4	1e-5	1e-4	3e-4	4e-4	1e-3	0.197	0.199	0.203	0.207	0.215	0.224	0.231	0.250
p_4	3e-4	6e-5	7e-5	8e-5	2e-4	3e-4	4e-4	1e-3	0.199	0.205	0.211	0.218	0.229	0.243	0.255	0.286
p_5	2e-4	1e-4	1e-4	3e-5	1e-4	4e-4	9e-4	3e-3	0.202	0.213	0.223	0.233	0.249	0.268	0.283	0.326

TABLE 4. Effects of the DAS on put option pricing in the Heston model.

We observe especially for scenarios p_4 and p_5, where the volatility of volatility ξ and correlation ρ have higher values, that the DAS has the strongest effect. Note that here we fix $r = 5\%$ as a particular case to highlight the de-Americanization effect, and we refer to [11] for a more detailed parameter study.

6.3. **Comparison between RBM and DAS.** Next, we perform a numerical comparison of the calibration with American put options using both model reduction techniques. That is, we consider the minimization problems (4.1) and (5.1). For comparative purposes, we also carry out the calibration with the detailed finite element solution (3.17).

First, we use a synthetic set of observations P^{obs} given by (6.3). We consider different parameter scenarios corresponding to different values of $\boldsymbol{\Theta} \in \mathcal{P}_{\mathrm{opt}}$; see Table 5. For each scenario, we construct an artificial set of observations $P_i^{\mathrm{obs}} := P_i^{\mathcal{N},\mathrm{Am}}$, $i = 1, \ldots, 65$. In general, the parameter κ is price-insensitive, see, e.g., [38], and thus it cannot be reconstructed. Therefore, we fix κ to its exact value and do the parameter estimation only for ξ, ρ, γ, and ν_0. The results of the calibration are summarized in Tables 6 and 7. We observe that, overall, all methods provide a good reconstruction of the parameters. As can be expected, the most cost-intense variant also provides the results with the highest accuracy. However all of our surrogate models yield quite good results.

We observe that both reduction approaches provide a significant speed-up compared to the expensive detailed solver, which on average takes about eight hours for each scenario. Although the DAS allows for an extremely efficient calibration process, it requires an additional pre-processing step for the data. In contrast to the RBM, this pre-processing

	ξ	ρ	γ	κ	ν_0
p_1	0.10	-0.20	0.07	0.5	0.07
p_2	0.25	-0.50	0.10	0.5	0.10
p_3	0.40	-0.50	0.15	0.6	0.15
p_4	0.55	-0.45	0.20	1.2	0.20
p_5	0.70	-0.80	0.30	1.4	0.30
p_6	0.2928	-0.7571	0.0707	0.6067	0.0707

TABLE 5. Overview of the parameter sets used to generate the synthetic data set

Scenario	Method	$\mathbb{E}(\boldsymbol{\mu})$	$\#J$	calib. time	pre-process. time for P^{obs}
p_1	$J_{\mathcal{N}}(\boldsymbol{\Theta})$	$\mathbb{E}_{\mathcal{N}}^{\text{Am}}$	75	8.524 hrs	36.045 min
	$\widetilde{J}_{\mathcal{N}}(\boldsymbol{\Theta})$	$\mathbb{E}_{\mathcal{N}}^{\text{Eu}}$	145	18.018 min	
	$J_N(\boldsymbol{\Theta})$	$\mathbb{E}_N^{\text{Am}}$	70	3.912 min	
p_2	$J_{\mathcal{N}}(\boldsymbol{\Theta})$	$\mathbb{E}_{\mathcal{N}}^{\text{Am}}$	65	8.035 hrs	36.830 min
	$\widetilde{J}_{\mathcal{N}}(\boldsymbol{\Theta})$	$\mathbb{E}_{\mathcal{N}}^{\text{Eu}}$	70	8.895 min	
	$J_N(\boldsymbol{\Theta})$	$\mathbb{E}_N^{\text{Am}}$	70	3.489 min	
p_3	$J_{\mathcal{N}}(\boldsymbol{\Theta})$	$\mathbb{E}_{\mathcal{N}}^{\text{Am}}$	60	8.341 hrs	35.374 min
	$\widetilde{J}_{\mathcal{N}}(\boldsymbol{\Theta})$	$\mathbb{E}_{\mathcal{N}}^{\text{Eu}}$	60	8.083 min	
	$J_N(\boldsymbol{\Theta})$	$\mathbb{E}_N^{\text{Am}}$	70	3.574 min	
p_4	$J_{\mathcal{N}}(\boldsymbol{\Theta})$	$\mathbb{E}_{\mathcal{N}}^{\text{Am}}$	50	7.088 hrs	36.660 min
	$\widetilde{J}_{\mathcal{N}}(\boldsymbol{\Theta})$	$\mathbb{E}_{\mathcal{N}}^{\text{Eu}}$	45	6.031 min	
	$J_N(\boldsymbol{\Theta})$	$\mathbb{E}_N^{\text{Am}}$	55	2.813 min	
p_5	$J_{\mathcal{N}}(\boldsymbol{\Theta})$	$\mathbb{E}_{\mathcal{N}}^{\text{Am}}$	40	6.331 hrs	36.574 min
	$\widetilde{J}_{\mathcal{N}}(\boldsymbol{\Theta})$	$\mathbb{E}_{\mathcal{N}}^{\text{Eu}}$	65	8.607 min	
	$J_N(\boldsymbol{\Theta})$	$\mathbb{E}_N^{\text{Am}}$	45	2.271 min	
p_6	$J_{\mathcal{N}}(\boldsymbol{\Theta})$	$\mathbb{E}_{\mathcal{N}}^{\text{Am}}$	70	9.665 hrs	36.960 min
	$\widetilde{J}_{\mathcal{N}}(\boldsymbol{\Theta})$	$\mathbb{E}_{\mathcal{N}}^{\text{Eu}}$	70	9.555 min	
	$J_N(\boldsymbol{\Theta})$	$\mathbb{E}_N^{\text{Am}}$	90	4.503 min	

TABLE 6. Computational time for calibrating American put options using different model reduction techniques.

depends on the actual market data and therefore can not be performed in advance. This is a serious bottleneck compared to the RBM approach.

Figure 3 shows the influence of the different calibration approaches on the parameters. It can be seen that in all approaches the main difficulty arises in in identifying ξ and ρ. In fact, this tendency has been also observed for the detailed solver (see cases p_1, p_4, Table 7). The remaining parameters γ and ν_0 are recovered almost exactly. We also note that for scenarios p_1–p_3, which correspond to the cases when ξ, ν_0 and ρ are the smallest, the DAS calibration is able to provide a better reconstruction of the parameter ξ than the RBM. By contrast, in the scenarios p_4 and p_5, which correspond to large values of the correlation parameter, the DAS gives poorer results for ξ and ρ. This is consistent with the observation made in Section 5, where we noticed that the errors caused by de-Americanization are the largest in the cases where ξ and ρ are large (see Table 4, scenario p_5, maturity T_8).

Scenario	Method	$\mathbb{E}(\boldsymbol{\mu})$	$\boldsymbol{\Theta}$	ξ	ρ	γ	ν_0	$J(\boldsymbol{\Theta}^\star)$
			$\boldsymbol{\Theta}_{\text{ex}}$	0.1	-0.2	0.07	0.07	
p_1	$J_{\mathcal{N}}(\boldsymbol{\Theta})$	$\mathbb{E}_{\mathcal{N}}^{\text{Am}}$	$\boldsymbol{\Theta}^\star$	0.1002	-0.1997	0.07	0.07	7.8806e-14
	$\widetilde{J}_{\mathcal{N}}(\boldsymbol{\Theta})$	$\mathbb{E}_{\mathcal{N}}^{\text{Eu}}$	$\boldsymbol{\Theta}^\star$	0.1000	-0.3003	0.0701	0.0688	1.0248e-07
	$J_N(\boldsymbol{\Theta})$	$\mathbb{E}_N^{\text{Am}}$	$\boldsymbol{\Theta}^\star$	0.1477	-0.0788	0.0697	0.0700	4.3440e-08
			$\boldsymbol{\Theta}_{\text{ex}}$	0.25	-0.5	0.1	0.1	
p_2	$J_{\mathcal{N}}(\boldsymbol{\Theta})$	$\mathbb{E}_{\mathcal{N}}^{\text{Am}}$	$\boldsymbol{\Theta}^\star$	0.25	-0.5	0.1	0.1	6.4756e-17
	$\widetilde{J}_{\mathcal{N}}(\boldsymbol{\Theta})$	$\mathbb{E}_{\mathcal{N}}^{\text{Eu}}$	$\boldsymbol{\Theta}^\star$	0.2404	-0.5388	0.1001	0.0991	1.1363e-08
	$J_N(\boldsymbol{\Theta})$	$\mathbb{E}_N^{\text{Am}}$	$\boldsymbol{\Theta}^\star$	0.2860	-0.4824	0.0968	0.1015	9.9148e-08
			$\boldsymbol{\Theta}_{\text{ex}}$	0.4	-0.5	0.15	0.15	
p_3	$J_{\mathcal{N}}(\boldsymbol{\Theta})$	$\mathbb{E}_{\mathcal{N}}^{\text{Am}}$	$\boldsymbol{\Theta}^\star$	0.4	-0.5	0.15	0.15	2.9834e-18
	$\widetilde{J}_{\mathcal{N}}(\boldsymbol{\Theta})$	$\mathbb{E}_{\mathcal{N}}^{\text{Eu}}$	$\boldsymbol{\Theta}^\star$	0.4282	-0.4620	0.1544	0.1492	2.2003e-09
	$J_N(\boldsymbol{\Theta})$	$\mathbb{E}_N^{\text{Am}}$	$\boldsymbol{\Theta}^\star$	0.3537	-0.5731	0.1456	0.1504	6.2085e-09
			$\boldsymbol{\Theta}_{\text{ex}}$	0.55	-0.45	0.2	0.2	
p_4	$J_{\mathcal{N}}(\boldsymbol{\Theta})$	$\mathbb{E}_{\mathcal{N}}^{\text{Am}}$	$\boldsymbol{\Theta}^\star$	0.5502	-0.4499	0.2	0.2	4.8235e-14
	$\widetilde{J}_{\mathcal{N}}(\boldsymbol{\Theta})$	$\mathbb{E}_{\mathcal{N}}^{\text{Eu}}$	$\boldsymbol{\Theta}^\star$	0.5801	-0.4220	0.2044	0.1989	1.5377e-09
	$J_N(\boldsymbol{\Theta})$	$\mathbb{E}_N^{\text{Am}}$	$\boldsymbol{\Theta}^\star$	0.5048	-0.4980	0.1989	0.1995	1.6681e-08
			$\boldsymbol{\Theta}_{\text{ex}}$	0.7	-0.8	0.3	0.3	
p_5	$J_{\mathcal{N}}(\boldsymbol{\Theta})$	$\mathbb{E}_{\mathcal{N}}^{\text{Am}}$	$\boldsymbol{\Theta}^\star$	0.7	-0.8	0.3	0.3	3.4388e-18
	$\widetilde{J}_{\mathcal{N}}(\boldsymbol{\Theta})$	$\mathbb{E}_{\mathcal{N}}^{\text{Eu}}$	$\boldsymbol{\Theta}^\star$	0.8433	-0.6668	0.3170	0.2990	1.8369e-08
	$J_N(\boldsymbol{\Theta})$	$\mathbb{E}_N^{\text{Am}}$	$\boldsymbol{\Theta}^\star$	0.6881	-0.8259	0.2994	0.3006	1.0533e-08
			$\boldsymbol{\Theta}_{\text{ex}}$	0.2928	-0.7571	0.0707	0.0707	
p_6	$J_{\mathcal{N}}(\boldsymbol{\Theta})$	$\mathbb{E}_{\mathcal{N}}^{\text{Am}}$	$\boldsymbol{\Theta}^\star$	0.2928	0.7571	0.0707	0.0707	6.5746e-18
	$\widetilde{J}_{\mathcal{N}}(\boldsymbol{\Theta})$	$\mathbb{E}_{\mathcal{N}}^{\text{Eu}}$	$\boldsymbol{\Theta}^\star$	0.3690	-0.6026	0.0736	0.0685	1.6179e-07
	$J_N(\boldsymbol{\Theta})$	$\mathbb{E}_N^{\text{Am}}$	$\boldsymbol{\Theta}^\star$	0.3096	-0.7049	0.0700	0.0718	9.6369e-08

TABLE 7. Calibration results on the synthetic data set of American put options in the Heston model with different model reduction techniques: the RBM, the de-Americanization method and the detailed problem.

To summarize our findings, the cases with "extreme" parameter values have a significant impact on the performance of the optimization routine, in both the detailed and the reduced problems. In the case of the reduced basis method, this difficulty may be overcome for example by considering an adaptive parameter domain partition [29], in particular for ξ and ρ, or by increasing the number of snapshots, and furthermore by increasing the dimension of the reduced system. However, this will also result in an increase in the time required to compute the solution.

6.4. **Real market data.** Finally, we extend our approach to the calibration of a real market data set, provided by options on the Google stock. Since the Google stock does not pay dividends, the American call options can be priced the same as the European call options, [36]. Hence, we restrict consideration to only American put options. Namely, we consider the data P^{obs} of 401 American put options with $S_0 = 523.755$, $r = 0.15\%$ on February 2nd, 2015. The data is pre-processed using the methodology applied to the volatility index (VIX) by the Chicago board of exchange [14]:

- For each option with strike price K_i, we consider the midpoint of the bid-ask spread.
- Options with zero bid prices are neglected.

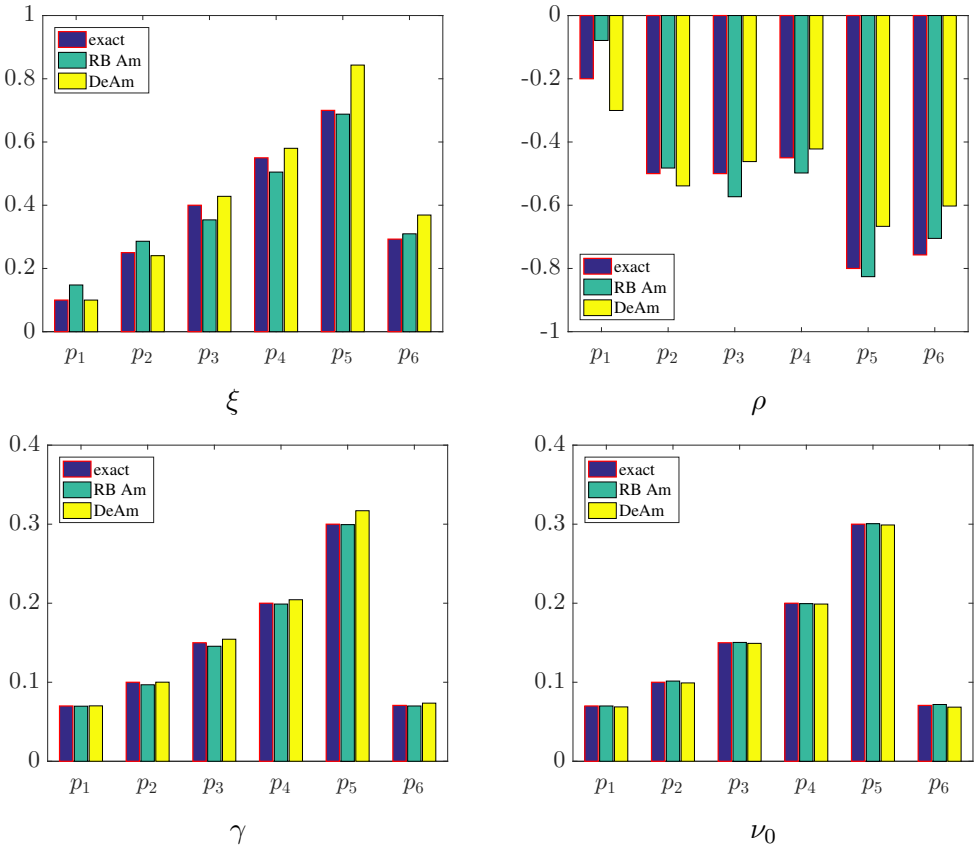

FIGURE 3. Reconstructed parameters for the different scenarios obtained by calibrating American put options with different model reduction techniques.

- If two puts with consecutive strike prices have zero bid prices, no puts with lower strike prices are included.

The used data is given in the appendix, see Table 10. In terms of the moneyness, we consider all types, out-of-the money ($K_i < S_0$), at-the-money ($K_i = S_0$) and in-the-money ($K_i > S_0$) options.

In our synthetic test scenarios, the Feller condition (3.2) was automatically satisfied. However, this does not hold for general calibration processes. Thus, we impose the following additional constraint on $\boldsymbol{\Theta} = (\xi, \rho, \gamma, \kappa, \nu_0) \in \mathcal{P}_{\text{opt}}$

$$\mathcal{P}_{\text{opt}} := \left\{ \boldsymbol{\Theta} \in \mathbb{R}^5 : \Theta_{\min,i} \leq \Theta_i \leq \Theta_{\max,i}, \quad 2\Theta_3\Theta_4 - \Theta_1^2 < 0, \quad i = 1, \ldots, 5 \right\}. \tag{6.4}$$

As optimization algorithm, we take the MATLAB function *fmincon* based on the Interior-Point method and which, in contrast to *lsqnonlin*, allows the inclusion of inequality constraints. We consider the same termination condition for the optimization routine as previously.

To calibrate the parameters, we consider the detailed minimization problem (3.17) and, as previously, the reduced models: the RBM (4.1), the DAS (5.1) and the combination of both (5.3). For completeness, we also consider the calibration of the de-Americanized data using the closed-form solution of (5.2).

Method	$\mathbb{E}(\boldsymbol{\mu})$	$\boldsymbol{\Theta}$	ξ	ρ	γ	κ	ν_0
		$\boldsymbol{\Theta}_{\text{in}}$	0.6005	-0.6815	0.4867	2.02	0.4961
$J_{\mathcal{N}}(\boldsymbol{\Theta})$	$\mathbb{E}^{\text{Am}}_{\mathcal{N}}$	$\boldsymbol{\Theta}^\star$	0.5953	-0.7210	0.0527	3.3615	0.0584
$J_{N}(\boldsymbol{\Theta})$	$\mathbb{E}^{\text{Am}}_{N}$	$\boldsymbol{\Theta}^\star$	0.5144	-0.7964	0.0521	2.5906	0.0554
$\widetilde{J}_{\mathcal{N}}(\boldsymbol{\Theta})$	$\mathbb{E}^{\text{Eu}}_{\mathcal{N}}$	$\boldsymbol{\Theta}^\star$	0.4095	-0.6818	0.0516	1.6262	0.0567
$\widetilde{J}_{\text{CF}}(\boldsymbol{\Theta})$		$\boldsymbol{\Theta}^\star$	0.3927	-0.6518	0.0580	1.4554	0.0546

TABLE 8. Parameters obtained by the calibration on American put options given on the Google stock using different methods

The results of the calibration are presented in Table 8. As before, γ and ν_0 can be easily identified by all our approaches. The rate of mean reversion κ appears to be a non-identifiable parameter, and all models provide quite different results. For the remaining parameters ξ and ρ, we observe that the DAS tends to underestimate the volatility of volatility ξ and the correlation ρ, compared to the detailed and RBM approach. This is clearly reflected in all models that use the perturbed de-Americanized data, i.e., $\widetilde{J}_{\mathcal{N}}(\boldsymbol{\Theta})$ and $\widetilde{J}_{\text{CF}}(\boldsymbol{\Theta})$. This is in good agreement with our observations for the synthetic data sets (see scenario p_5 and p_6), wherefor large (absolute) values of the correlation parameters the DAS was unable to provide a good reconstruction of the parameters ξ and ρ.

Method	$\mathbb{E}(\boldsymbol{\mu})$	# iter.	# J	calib. time	pre-process. time for P^{obs}
$J_{\mathcal{N}}(\boldsymbol{\Theta})$	$\mathbb{E}^{\text{Am}}_{\mathcal{N}}$	35	219	68.72 hrs	
$J_{N}(\boldsymbol{\Theta})$	$\mathbb{E}^{\text{Am}}_{N}$	38	260	44.20 min	
$\widetilde{J}_{\mathcal{N}}(\boldsymbol{\Theta})$	$\mathbb{E}^{\text{Eu}}_{\mathcal{N}}$	34	207	56.47 min	4.96 hrs
$\widetilde{J}_{\text{CF}}(\boldsymbol{\Theta})$		43	265	4.30 min	4.96 hrs

TABLE 9. Computational time for calibrating American put options given on the Google stock in the Heston model using different methods

The results of the run-time performance of the different methods is given in Table 9. We observe that the detailed approach is much more cost-intense than the proposed surrogate models. The cost can be drastically reduced from a couple of days to less than an hour. Notably, we observe the substantial speed-up obtained by evaluating model prices with the closed-form solutions. This approach appears to us the most efficient when dealing with European options. However, taking into consideration the additional time for pre-processing the data in the DAS, the total time for calibration with this method can be much slower than the calibration with American options using the RBM, depending how often the calibration has to be performed with new market data. However, the DAS pre-processing time could be sped up by implementing more advanced tree methods. We also note that, in contrast to the DAS, the RBM approach allows us to control the accuracy by increasing the dimension of the reduced spaces.

Figure 4 shows the calibration results based on market data for the detailed and the RBM approaches and the results for the two DAS are provided in Figure 5. The relative error for all approaches does not exceed 50% and increases in the out-of-the money region, which corresponds to the smallest option prices. To reduce this effect, one could consider different weights in the objective functional, e.g., imposing larger weights for small option price values.

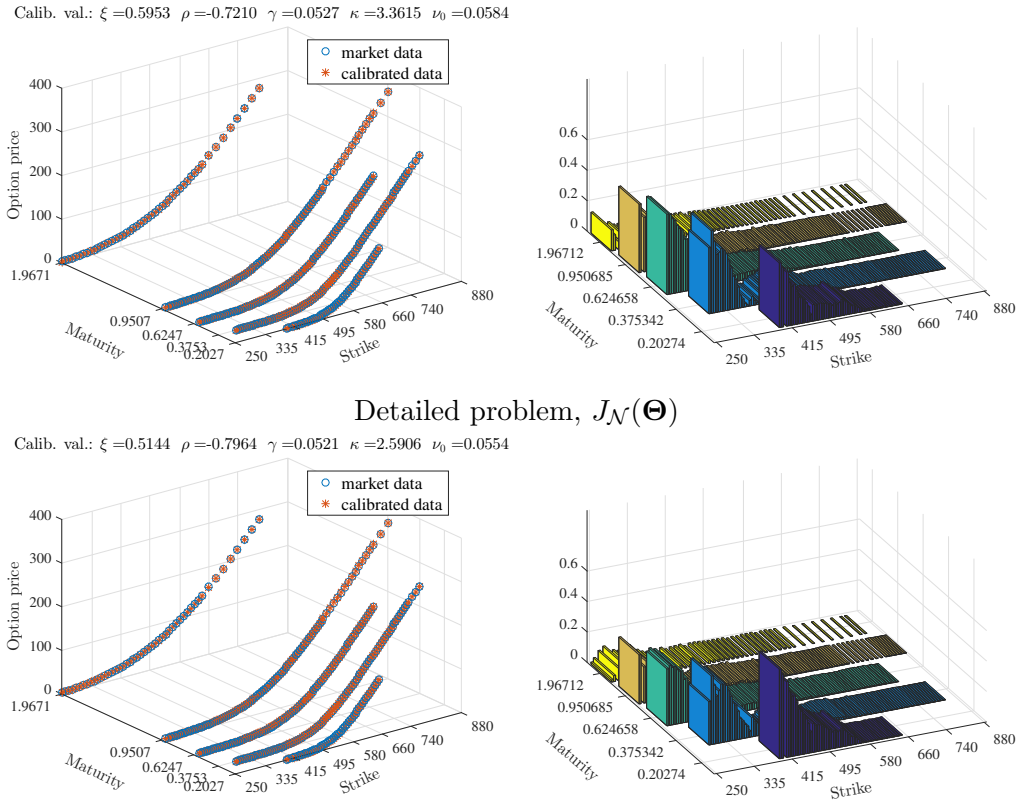

FIGURE 4. Left: the Google data set of American put options (circles) and the calibrated model data in the Heston model (stars). Right: the relative error of the market and calibrated data, $|P_i^{\text{obs}} - P_i^{s,\text{Am}}(\mathbf{\Theta}^\star)|/P_i^{\text{obs}}$, $i = 1, \ldots, M$, $s = \{\mathcal{N}, N\}$

7. Conclusion

In this paper, we applied the reduced basis methodology to the calibration of European and American put options. In the case of American options we additionally considered a de-Americanization strategy. Both reduction strategies are compared numerically. While RBM techniques aim to achieve smaller dimensions for the discrete spaces in the variational formulations of the problem, the DAS replaces the constrained PDE model of an American option with the unconstrained model of a European option. By doing so, a model error of fixed size occurs, but the RBM offer flexibility by allowing us to adaptively adjust the accuracy.

References

[1] Y. Achdou, *An inverse problem for a parabolic variational inequality arising in volatility calibration with American options*, SIAM J. Control Optim., 43 (2005), pp. 1583–1615 (electronic), doi:10.1137/S0363012903424423.

[2] Y. Achdou and O. Pironneau, *Computational methods for option pricing*, vol. 30 of Frontiers in Applied Mathematics, Society for Industrial and Applied Mathematics (SIAM), Philadelphia, PA, 2005, doi:10.1137/1.9780898717495.

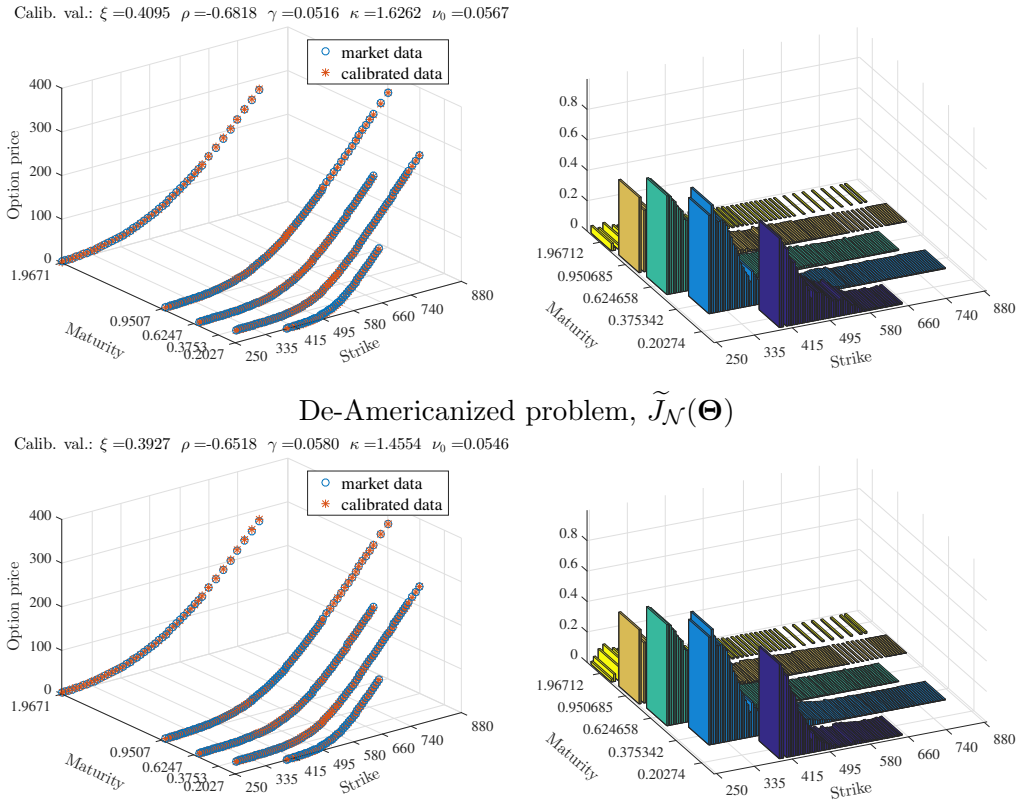

FIGURE 5. Left: the Google data set of the de-Americanized American put options (circles) and the calibrated model data in the Heston model (stars). Right: the relative error of the market and calibrated data, $|P_i^{\mathrm{obs}} - P_i^{s,\mathrm{Eu}}(\boldsymbol{\Theta}^\star)|/P_i^{\mathrm{obs}}$, $i = 1, \ldots, M$, $s = \{\mathcal{N}, \mathrm{CF}\}$

[3] Y. ACHDOU AND O. PIRONNEAU, *Numerical procedure for calibration of volatility with American options*, Applied Mathematical Finance, 12 (2005), pp. 201–241, doi:10.1080/1350486042000297252.

[4] M. BALAJEWICZ, D. AMSALLEM, AND C. FARHAT, *Projection-based model reduction for contact problems*, 2016, doi:10.1002/nme.5135.

[5] M. BALAJEWICZ AND J. TOIVANEN, *Reduced order models for pricing American options under stochastic volatility and jump-diffusion models*, Procedia Computer Science, 80 (2016), pp. 734–743, doi:10.1016/j.procs.2016.05.360. International Conference on Computational Science 2016, ICCS 2016, 6-8 June 2016, San Diego, California, USA.

[6] F. BLACK AND M. SCHOLES, *The pricing of options and corporate liabilities*, J. Polit. Econ., 81 (1973), pp. 637–654, doi:10.1086/260062.

[7] I. BOUCHOUEV AND V. ISAKOV, *The inverse problem of option pricing*, Inverse Problems, 13 (1997), pp. L11–L17, doi:10.1088/0266-5611/13/5/001.

[8] F. BREZZI, W. W. HAGER, AND P.-A. RAVIART, *Error estimates for the finite element solution of variational inequalities. II. Mixed methods*, Numer. Math., 31 (1978/79), pp. 1–16, doi:10.1007/BF01396010.

[9] M. BROADIE AND P. GLASSERMAN, *Pricing American-style securities using simulation*, J. Econom. Dynam. Control, 21 (1997), pp. 1323–1352, doi:10.1016/S0165-1889(97)00029-8.

[10] O. BURKOVSKA, *Reduced Basis Methods for Option Pricing and Calibration*, PhD thesis, Technische Universität München, 2016.

[11] O. Burkovska, K. Glau, M. Gass, M. Mahlstedt, W. Schoutens, and B. Wohlmuth, *Calibration to American options: Numerical investigation of the de-Americanization method*. Working paper, in preparation, 2016.
[12] O. Burkovska, B. Haasdonk, J. Salomon, and B. Wohlmuth, *Reduced basis methods for pricing options with the Black-Scholes and Heston models*, SIAM J. Financial Math., 6 (2015), pp. 685–712, doi:10.1137/140981216.
[13] P. Carr and L. Wu, *Stock options and credit default swaps: A joint framework for valuation and estimation*, Journal of Financial Econometrics, 8 (2010), pp. 409–449, doi:10.1093/jjfinec/nbp010.
[14] CBOE, *The CBOE volatility index – VIX*, CBOE, (2009).
[15] N. Clarke and K. Parrott, *Multigrid for American option pricing with stochastic volatility*, Applied Mathematical Finance, 6 (1999), pp. 177–195, doi:10.1080/135048699334528.
[16] R. Cont, N. Lantos, and O. Pironneau, *A reduced basis for option pricing*, SIAM J. Financial Math., 2 (2011), pp. 287–316, doi:10.1137/10079851X.
[17] J. Cox, *Notes on option pricing I: Constant elasticity of variance diffusions*, Unpublished note, Stanford University, Graduate School of Business, (1975).
[18] J. C. Cox, S. A. Ross, and M. Rubinstein, *Option pricing: A simplified approach*, Journal of Financial Economics, 7 (1979), pp. 229–263, doi:10.1016/0304-405X(79)90015-1.
[19] M. A. Dihlmann and B. Haasdonk, *Certified PDE-constrained parameter optimization using reduced basis surrogate models for evolution problems*, Comput. Optim. Appl., 60 (2015), pp. 753–787, doi:10.1007/s10589-014-9697-1.
[20] B. Düring and M. Fournié, *High-order compact finite difference scheme for option pricing in stochastic volatility models*, J. Comput. Appl. Math., 236 (2012), pp. 4462–4473, doi:10.1016/j.cam.2012.04.017.
[21] H. Egger and H. W. Engl, *Tikhonov regularization applied to the inverse problem of option pricing: convergence analysis and rates*, Inverse Problems, 21 (2005), pp. 1027–1045, doi:10.1088/0266-5611/21/3/014.
[22] F. Fang and C. W. Oosterlee, *A Fourier-based valuation method for Bermudan and barrier options under Heston's Model*, SIAM Journal of Financial Mathematics, 2 (2011), pp. 439–463.
[23] S. Figlewski and X. Wang, *Is the 'leverage effect' a leverage effect?*, Available at SSRN 256109, (2000), doi:10.2139/ssrn.256109.
[24] M. C. Fu, S. B. Laprise, D. B. Madan, Y. Su, and R. Wu, *Pricing American options: A comparison of Monte Carlo simulation approaches*, Journal of Computational Finance, 4 (2001), pp. 39–88, doi:10.21314/JCF.2001.066.
[25] F. Gerlich, A. M. Giese, J. H. Maruhn, and E. W. Sachs, *Parameter identification in financial market models with a feasible point SQP algorithm*, Comput. Optim. Appl., 51 (2012), pp. 1137–1161, doi:10.1007/s10589-010-9369-8.
[26] S. Glas and K. Urban, *On noncoercive variational inequalities*, SIAM J. Numer. Anal., 52 (2014), pp. 2250–2271, doi:10.1137/130925438.
[27] M. A. Grepl, *Reduced-basis approximation and a posteriori error estimation for parabolic partial differential equations*, PhD thesis, Massachusetts Institute of Technology, 2005.
[28] B. Haasdonk, *Convergence rates of the POD-greedy method*, ESAIM Math. Model. Numer. Anal., 47 (2013), pp. 859–873, doi:10.1051/m2an/2012045.
[29] B. Haasdonk, M. Dihlmann, and M. Ohlberger, *A training set and multiple bases generation approach for parameterized model reduction based on adaptive grids in parameter space*, Math. Comput. Model. Dyn. Syst., 17 (2011), pp. 423–442, doi:10.1080/13873954.2011.547674.
[30] B. Haasdonk and M. Ohlberger, *Reduced basis method for finite volume approximations of parametrized linear evolution equations*, M2AN Math. Model. Numer. Anal., 42 (2008), pp. 277–302, doi:10.1051/m2an:2008001.
[31] B. Haasdonk, J. Salomon, and B. Wohlmuth, *A reduced basis method for parametrized variational inequalities*, SIAM J. Numer. Anal., 50 (2012), pp. 2656–2676, doi:10.1137/110835372.
[32] J. S. Hesthaven, G. Rozza, and B. Stamm, *Certified reduced basis methods for parametrized partial differential equations*, SpringerBriefs in Mathematics, Springer, Cham; BCAM Basque Center for Applied Mathematics, Bilbao, 2016, doi:10.1007/978-3-319-22470-1. BCAM SpringerBriefs.
[33] S. L. Heston, *A closed-form solution for options with stochastic volatility with applications to bond and currency options*, The Review of Financial Studies, 6 (1993), pp. 327–43, doi:10.1093/rfs/6.2.327.
[34] N. Hilber, O. Reichmann, C. Schwab, and C. Winter, *Computational methods for quantitative finance. Finite element methods for derivative pricing.*, Springer Finance, 2013, doi:10.1007/978-3-642-35401-4.

[35] M. Hintermüller, *Inverse coefficient problems for variational inequalities: optimality conditions and numerical realization*, M2AN Math. Model. Numer. Anal., 35 (2001), pp. 129–152, doi:10.1051/m2an:2001109.
[36] J. C. Hull, *Options, Futures, and Other Derivative Securities*, Prentice-Hall, fifth ed., 2003.
[37] K. Ito and K. Kunisch, *Optimal control of elliptic variational inequalities*, Appl. Math. Optim., 41 (2000), pp. 343–364, doi:10.1007/s002459911017.
[38] A. Janek, T. Kluge, R. Weron, and U. Wystup, *FX smile in the Heston model*, in Statistical tools for finance and insurance, Springer, Heidelberg, 2011, pp. 133–162, doi:10.1007/978-3-642-18062-0_4.
[39] N. Kikuchi and J. T. Oden, *Contact problems in elasticity: a study of variational inequalities and finite element methods*, vol. 8 of SIAM Studies in Applied Mathematics, Society for Industrial and Applied Mathematics (SIAM), Philadelphia, PA, 1988, doi:10.1137/1.9781611970845.
[40] D. D. Lee and H. S. Seung, *Learning the parts of objects by non-negative matrix factorization*, Nature, 401 (1999), pp. 788–791, doi:10.1038/44565.
[41] S. Z. Levendorskiĭ, *Early exercise boundary and option prices in Lévy driven models*, Quantitative Finance, 4 (2004), pp. 525–547.
[42] F. A. Longstaff and E. S. Schwartz, *Valuing american options by simulation: a simple least-squares approach*, Review of Financial studies, 14 (2001), pp. 113–147, doi:10.1093/rfs/14.1.113.
[43] A. Mayerhofer and K. Urban, *A reduced basis method for parabolic partial differential equations with parameter functions and application to option pricing*. Preprint, University of Ulm, 2014, arXiv:1408.2709. accepted for publication in Journal of Computational Finance.
[44] M. Mrázek, J. Pospíšil, and T. Sobotka, *On optimization techniques for calibration of stochastic volatility models*, in AMCM 2015, November 28–30, 2014, Athens, Greece, 2014, pp. 34–40, `http://www.inase.org/library/2014/athens/bypaper/APPLIED/APPLIED-04.pdf`.
[45] A. T. Patera and G. Rozza, *Reduced basis approximation and a posteriori error estimation for parametrized partial differential equations*, Tech. Report Version 1.0, MIT 2006–2007, to appear in (tentative rubric) MIT Pappalardo Graduate Monographs in Mechanical Engineering, Massachusetts Institute of Technology, 2006, `http://augustine.mit.edu/methodology/bookParts/Patera_Rozza_bookPartI_BV1.pdf`.
[46] B. Peherstorfer, P. Gómez, and H.-J. Bungartz, *Reduced models for sparse grid discretizations of the multi-asset Black-Scholes equation*, Advances in Computational Mathematics, 41 (2015), pp. 1365–1389, doi:10.1007/s10444-015-9421-4.
[47] O. Pironneau, *Calibration of options on a reduced basis*, J. Comput. Appl. Math., 232 (2009), pp. 139–147, doi:10.1016/j.cam.2008.10.070.
[48] O. Pironneau, *Reduced basis for vanilla and basket options*, Risk and Decision Analysis, 2 (2011), pp. 185–194, doi:10.3233/RDA-2011-0045.
[49] O. Pironneau, *Proper orthogonal decomposition for pricing options*, Journal of Computational Finance, 16 (2012), pp. 33–46, doi:10.21314/JCF.2012.246.
[50] A. Quarteroni, A. Manzoni, and F. Negri, *Reduced basis methods for partial differential equations*, vol. 92 of Unitext, Springer, Cham, 2016, doi:10.1007/978-3-319-15431-2. An introduction, La Matematica per il 3+2.
[51] A. Quarteroni and A. Valli, *Numerical approximation of partial differential equations*, vol. 23 of Springer Series in Computational Mathematics, Springer-Verlag, Berlin, 1994.
[52] L. C. G. Rogers, *Monte Carlo valuation of American options*, Math. Finance, 12 (2002), pp. 271–286, doi:10.1111/1467-9965.02010.
[53] D. Rovas, *Reduced-basis output bound methods for parametrized partial differential equations*, PhD thesis, Massachusetts Institute of Technology, 2003.
[54] G. Rozza and K. Veroy, *On the stability of the reduced basis method for Stokes equations in parametrized domains*, Comput. Methods Appl. Mech. Engrg., 196 (2007), pp. 1244–1260, doi:10.1016/j.cma.2006.09.005.
[55] M. Rubinstein, *Implied binomial trees*, The Journal of Finance, 49 (1994), pp. 771–818, doi:10.2307/2329207.
[56] E. W. Sachs and M. Schneider, *Reduced-order models for the implied variance under local volatility*, Int. J. Theor. Appl. Finance, 17 (2014), pp. 1450053, 23, doi:10.1142/S0219024914500538.
[57] E. W. Sachs, M. Schneider, and M. Schu, *Adaptive trust-region POD methods in PIDE-constrained optimization*, in Trends in PDE constrained optimization, vol. 165 of Internat. Ser. Numer. Math., Birkhäuser/Springer, Cham, 2014, pp. 327–342, doi:10.1007/978-3-319-05083-6_20.

[58] E. W. Sachs and M. Schu, *Reduced order models (POD) for calibration problems in finance*, in Numerical Mathematics and Advanced Applications: Proceedings of ENUMATH 2007, the 7th European Conference on Numerical Mathematics and Advanced Applications, Graz, Austria, September 2007, K. Kunisch, G. Of, and O. Steinbach, eds., Springer Berlin Heidelberg, Berlin, Heidelberg, 2008, pp. 735–742, doi:10.1007/978-3-540-69777-0_88.

[59] E. W. Sachs and S. Volkwein, *POD-Galerkin approximations in PDE-constrained optimization*, GAMM-Mitt., 33 (2010), pp. 194–208, doi:10.1002/gamm.201010015.

[60] A. Schiela and D. Wachsmuth, *Convergence analysis of smoothing methods for optimal control of stationary variational inequalities with control constraints*, ESAIM Math. Model. Numer. Anal., 47 (2013), pp. 771–787, doi:10.1051/m2an/2012049.

[61] W. Schoutens, E. Simons, and J. Tistaert, *A perfect calibration! Now what?*, Wilmott Magazine, (2004), pp. 66–78.

[62] B. Vexler, *Adaptive Finite Element Methods for Parameter Identification Problems*, PhD thesis, University of Heidelberg, 2004.

[63] B. I. Wohlmuth, *A mortar finite element method using dual spaces for the Lagrange multiplier*, SIAM J. Numer. Anal., 38 (2000), pp. 989–1012, doi:10.1137/S0036142999350929.

[64] Z. Zhang, E. Bader, and K. Veroy, *A slack approach to reduced-basis approximation and error estimation for variational inequalities*, C. R. Math. Acad. Sci. Paris, 354 (2016), pp. 283–289, doi:10.1016/j.crma.2015.10.024.

Appendix A. Google market data

$K\backslash T$	0.2027	0.3753	0.6247	0.9507	1.9671
250					2.50
260				1.20	2.90
265			0.55		
270			0.62	1.30	3.30
275			0.68	1.50	
280			0.75	1.62	3.80
285			0.80	1.73	
290			0.88	1.80	4.65
295			0.97	1.95	
300		0.28	1.00	2.10	5.35
305		0.40	1.12	2.27	
310		0.40	1.20	2.45	6.25
315		0.40	1.30	2.67	
320		0.47	1.38	2.85	7.40
325		0.57	1.50	3.12	
330		0.65	1.60	3.40	8.10
335		0.72	1.75	3.60	
340		0.78	1.90	3.85	9.65
345		0.82	2.05	4.20	
350		0.88	2.23	4.55	10.90
355		0.97	2.40	4.90	
360		1.05	2.70	5.30	12.55
365		1.12	2.90	5.65	
370		1.25	3.17	6.15	14.30
375		1.38	3.45	6.65	
380		1.52	3.75	7.15	16.45
385		1.65	4.10	7.65	
390		2.05	4.45	8.15	18.30
395	0.93	2.25	4.85	8.80	
400	1.05	2.50	5.30	9.45	20.85
405		2.73	5.75	10.10	
410	1.40	3.08	6.30	10.75	22.85
415	1.48	3.35	6.85	11.55	
420	1.65	3.75	7.45	12.40	25.55
425	1.93	4.10	8.15	13.40	
430	2.10	4.55	8.80	14.20	28.30
435	2.33	5.05	9.55	15.35	
440	2.70	5.55	10.40	16.25	31.35
445	3.10	6.10	11.25	17.35	
450	3.50	6.80	12.30	18.65	34.00
455	3.92	7.50	13.25	19.80	
460	4.25	8.35	14.25	21.20	37.80
465	5.20	9.20	15.45	22.60	
470	5.85	10.20	16.70	23.90	41.45
475	6.65	11.25	18.00	25.30	
480	7.60	12.40	19.45	27.15	45.20
485	8.65	13.70	20.95	28.55	
490	9.85	15.10	22.55	30.75	49.20
495	11.15	16.55	24.25	32.60	
500	12.65	18.25	26.00	34.60	53.50
505	14.05	20.00	27.90	36.80	
510	16.05	21.95	30.00	38.70	58.15
515	17.75	23.90	32.15	41.45	
520	19.90	26.20	34.40	43.65	62.90
525	22.50	28.55	36.70	46.05	
530	24.70	31.05	39.20	48.55	67.90
535	27.40	33.50	41.85	50.85	

$K\backslash T$	0.2027	0.3753	0.6247	0.9507	1.9671
540	30.20	36.40	44.45	52.70	72.65
545	33.25	39.25	47.60	56.10	
550	37.15	42.30	50.25	58.95	78.50
555	40.80	45.45	53.15	61.85	
560	44.30	49.00	56.55	64.80	84.05
565	48.25	52.35	59.40	67.50	
570	51.95	56.00	63.50	71.10	90.40
575	55.90	59.80	66.70	73.90	
580	60.20	63.70	69.85	77.25	96.45
585	64.50	67.10	74.25	81.30	
590	68.80	71.60	77.85	84.45	103.00
595	73.35	76.30	81.70	88.20	
600	77.35	80.65	85.10	91.55	108.85
605	82.35	84.80	89.65	95.20	
610	87.30	89.65	93.20	99.10	116.45
615	92.50	94.05	97.40	102.90	
620	96.65	98.45	101.85	106.80	123.75
625	101.30	103.00	106.40	111.80	
630	106.50	107.25	110.60	116.00	130.65
635	111.75	112.95	115.00	120.25	
640	117.20	117.25	119.85	124.40	138.10
645	121.45	122.30	124.40	128.55	
650	127.25	126.70	128.90	132.55	
655		131.45	133.70	137.15	
660		136.45	138.15	141.80	153.70
665		141.45	143.05	146.10	
670		146.65	147.35	150.50	
675		151.80	152.05	154.90	
680		156.20	158.25	159.45	169.45
685		161.20	161.60	164.05	
690		166.30	166.55	168.65	
695		171.30	171.45	173.15	
700		176.20	176.45	178.15	186.40
705		181.10	181.75		
710		186.15	186.25	188.40	
715		191.10	191.35		
720		196.05	195.85	197.15	203.70
725		201.05	201.80		
730		205.85	206.50	206.95	
735		211.00	211.05		
740		216.80	216.80	216.20	222.30
745		221.80	221.90		
750		226.55	226.85	226.20	
755		231.80			
760		236.80		236.15	240.60
765		241.95			
770		246.95		246.05	
775		251.80			
780		256.80		256.05	258.90
790		267.00		265.70	
800		276.95		276.05	277.70
810		287.25		286.05	
820				296.05	
830				306.05	
840				316.05	
860				336.05	
880				356.05	

Table 10. Google market data consisting of 401 American put options with $S_0 = 523,755$ on February 2nd, 2015.

O. Burkovska, Institute for Numerical Mathematics, Technische Universität München, 85748 Garching b. München, Germany

E-mail address: burkovsk@ma.tum.de

K. Glau, Chair of Mathematical Finance, Technische Universität München, 85748 Garching b. München, Germany

E-mail address: kathrin.glau@tum.de

M. Mahlstedt, Chair of Mathematical Finance, Technische Universität München, 85748 Garching b. München, Germany
E-mail address: mirco.mahlstedt@tum.de

B. Wohlmuth, Institute for Numerical Mathematics, Technische Universität München, 85748 Garching b. München, Germany
E-mail address: wohlmuth@ma.tum.de